

Spring 4-18-2019

Non-invasive beam monitoring with harmonic cavities

Brock F. Roberts
University of New Mexico

Follow this and additional works at: https://digitalrepository.unm.edu/ece_etds



Part of the [Electromagnetics and Photonics Commons](#)

Recommended Citation

Roberts, Brock F.. "Non-invasive beam monitoring with harmonic cavities." (2019). https://digitalrepository.unm.edu/ece_etds/459

This Dissertation is brought to you for free and open access by the Engineering ETDs at UNM Digital Repository. It has been accepted for inclusion in Electrical and Computer Engineering ETDs by an authorized administrator of UNM Digital Repository. For more information, please contact amywinter@unm.edu.

Brock Franklin Roberts

Candidate

Electrical and Computer Engineering

Department

This dissertation is approved, and it is acceptable in quality and form for publication:

Approved by the Dissertation Committee:

Edl Schamiloglu, Chairperson

Jim Ellison

Mark Gilmore

Christos Christodoulou

NON-INVASIVE BEAM MONITORING WITH HARMONIC CAVITIES

by

BROCK FRANKLIN ROBERTS

Bachelor of Science in Physics from the University of California at Davis, 1992

DISSERTATION

Submitted in Partial Fulfillment of the
Requirements for the Degree of

Doctor of Philosophy in Engineering

The University of New Mexico,
Albuquerque, New Mexico

May, 2019

DEDICATION

To my parents, Bill and Vali, for encouraging creativity.

ACKNOWLEDGEMENTS

This research effort has been accomplished because of the hard work, careful thinking, and generosity of many individuals at several institutions. All beamline work was done at the Thomas Jefferson National Accelerator Facility (TJNAF or Jlab), thanks to the curiosity and experimental genius of Matt Poelker and his team at the Center for Injectors and Sources (CIS), the co-authors of [1] and [2]. When I cold-called Matt in 2010, I was making harmonic cavities out of wood laminated with copper sheet and looking for accelerator applications. This led to a visit to Jlab, where Matt wondered aloud if a harmonic cavity could be used as a beam monitor, to which I replied, “What is a beam monitor?” By the end of the day we had concluded that the cavity’s antennas output would be related to the beams Fourier series. Matt challenged me to build a harmonic cavity compatible with the beamline, and it was off to the races. At the University of New Mexico; EdI Schamiloglu took me on as a PhD student for which I am tremendously grateful, and he along with Jim Ellison and Klaus Heinemann have provided encouragement and insight. Fellow graduate students Shawn Soh and Chris Leach created illuminating particle in cell models. At Electrodynamic; Don Speirs, Melcoy Pablo, and Art Sanchez devoted their time, brains, and hardworking hands to design and built apparatus, electronics, and software. This work was funded by Department of Energy’s Nuclear Physics (NP) Small Business Innovative Research program (SBIR), grant # DE-SC0009509, thanks NP, thanks everyone.

NON INVASIVE BEAM MONITORING WITH HARMONIC CAVITIES

by

Brock Franklin Roberts

B.S PHYSICS, UNIVERSITY OF CALIFORNIA DAVIS, 1992

DOCTOR OF PHILOSOPHY IN ELECTRICAL ENGINEERING

UNIVERSITY OF NEW MEXICO, 2019

ABSTRACT

A cavity designed to have multiple harmonic TM_{0N0} modes can be used to accurately measure the longitudinal profile of a bunched charged particle beam passing through its bore, non-invasively, and in real time.

Multi-harmonic TM_{0N0} cavities were designed, constructed, and beamline tested in a variety of experiments at the Thomas Jefferson National Accelerator Facility (TJNAF or Jlab). Measurements with a sampling oscilloscope provided signals that resemble the profile of electron bunches passing through the cavity's bore. Straightforward signal processing techniques reduce distortion in the measurement and provide real time profiles of electron bunches with picosecond accuracy. Subharmonic beams having bunch repetition rates of $1/3^{\text{rd}}$ and $1/6^{\text{th}}$ of Jlab's 1497 MHz bunch frequency, and interleaved sub-harmonic beams were also measured. Comparison between measurements made using a harmonic cavity were corroborated with an established invasive measurement method and with computer models. A harmonic cavity from this effort has been installed within the CEBAF injector, allowing accelerator operators to view, in real time, the shape and duration of electron bunches entering the accelerator. Another harmonic cavity has been installed within Jlab's Upgraded Injector Test Facility (UITF), and two more are planned for installation there. This effort was awarded the 2016 International Beam Instrumentation Conference's Faraday Cup Award.

TABLE OF CONTENTS

DEDICATION	iii
ACKNOWLEDGEMENTS.....	iv
ABSTRACT	vi
CHAPTER 1: INTRODUCTION	1
1.1 MULTI-HARMONIC TM_{0NO} CAVITIES	2
CHAPTER 2: MEASUREMENTS AT THE INJECTOR TEST FACILITY	10
2.1: The Injector Test Facility (ITF)	10
2.2 Harmonic cavity testing on the ITF beamline	11
2.3: The Discrete Fourier Transform (DFT) and the harmonic cavity's mode by mode response.....	13
2.4 Distortion in the harmonic cavity signal.....	14
2.5 An estimate of the harmonic cavity's transfer function	15
2.6 Measurements of Bulk GaAs and superlattice at 75 kV and 175 kV accelerating voltages	19
CHAPTER 3: MEASUREMENTS AT THE CONTINUOUS ELECTRON BEAM ACCELERATOR FACILITY (CEBAF).....	26
3.1: A 1497 MHz harmonic cavity.....	26
3.2 The CEBAF injector	26
3.3 Chopping a 499 MHz beam.....	27
3.4 The RF deflection technique	29
3.5: Measurements of the 499 MHz beam by the deflection technique.....	29
3.6: Measurements of the 499 MHz beam with a harmonic cavity.....	30

3.7: Measurements of the 249.5 MHz beam by the deflection technique.....	31
3.8: Measurements of the 249.5 MHz with a harmonic cavity	32
3.9 Measurement of an interleaved 499 MHz beams using a 1497 MHz harmonic cavity	33
3.10 Measuring interleaved bunch alignment with an RF detector	39
3.11 500 kV Measurements.....	40
CHAPTER 4 KEY CONCEPTS AND CONCLUSION	43
4.1 Subharmonic measurements	43
4.2 Key concepts	45
4.3 Conclusion.....	46
APPENDIX A: Faraday cup award	48
APPENDIX B: Publications.....	50
APPENDIX C: Design flowchart	51
APPENDIX D: Patent 9,385,412 for “Harmonic cavity resonator”	52
LIST OF REFERENCES.....	56

LIST OF FIGURES

- FIGURE 1.1.1: AN ILLUSTRATION OF THE SUPERPOSITION OF THE TM_{010} , TM_{020} , TM_{030} , AND TM_{040} RESONANT MODES AT A MOMENT OF SIMULTANEOUS ELECTRIC FIELD MAXIMUM. 2
- FIGURE 1.1.2: SOME OF THE CAVITY GEOMETRIES THAT HAVE HARMONIC TM_{0N0} MODES ARE SHOWN IN CROSS SECTION WITH A HORIZONTAL AXIS OF SYMMETRY AND BEAM TUBE. 4
- FIGURE 1.1.3: ELECTRIC FIELD SOLUTIONS FOR THE TM_{010} - TM_{080} MODES. 5
- FIGURE 1.1.4: THE TIME EVOLUTION OF THE SUPERIMPOSED MODES TM_{010} - TM_{080} FOR THE CAVITY IN FIGURE 1.1.3 WITH ITS AXIS OF SYMMETRY ORIENTED VERTICALLY. 6
- FIGURE 1.1.5: A BEAMLINER COMPATIBLE HARMONIC CAVITY CONSTRUCTED FOR TESTING ON THE JLAB INJECTOR TEST FACILITY. 7
- FIGURE 1.1.6: THE CAVITY OF FIGURE 1.1.5 SANDWICHED BETWEEN TWO 12" TO 2 $\frac{3}{4}$ " FLANGE REDUCERS TO MAKE IT COMPATIBLE WITH JLAB'S INJECTOR TEST FACILITY BEAMLINER. 8
- FIGURE 2.2.1: ONE WAVELENGTH OF THE HARMONIC CAVITY'S RESPONSE TO A 27 UA, 170 KV, 1533 MHZ BEAM CREATED USING A SUPERLATTICE PHOTOCATHODE. 12
- FIGURE 2.3.1: A GRAPH OF THE RELATIVE MAGNITUDE OF THE HARMONIC CAVITY RESONANCES EXCITED BY THE BEAM AND COUPLED TO THE OSCILLOSCOPE SHOWING THE FIRST 20 OF $N/2$ POSITIVE FREQUENCY TERMS. 13

FIGURE 2.5.1: AN ESTIMATE OF A 25 UA AND 175 KV BEAM'S LONGITUDINAL PROFILE.	18
FIGURE 2.6.1: HARMONIC CAVITY SIGNALS FOR A 25 UA, 75 KV BEAM.	19
FIGURE 2.6.2: PROCESSED SIGNALS FOR A 25 UA, 75 KV BEAM.	19
FIGURE 2.6.3: HARMONIC CAVITY SIGNALS FOR A 250 UA, 75 KV BEAM.	20
FIGURE 2.6.4: PROCESSED SIGNALS FOR A 250 UA, 75 KV BEAM.	20
FIGURE 2.6.5: HARMONIC CAVITY SIGNALS FOR A 500 UA, 75 KV BEAM.	21
FIGURE 2.6.6: PROCESSED SIGNALS FOR A 500 UA, 75 KV BEAM.	21
FIGURE 2.6.7: HARMONIC CAVITY SIGNALS FOR A 25 UA, 175 KV BEAM.	22
FIGURE 2.6.8: PROCESSED SIGNALS FOR A 25 UA, 175 KV BEAM.	22
FIGURE 2.6.9: HARMONIC CAVITY SIGNALS FOR A 250 UA, 175 KV BEAM.	23
FIGURE 2.6.10: PROCESSED SIGNALS FOR A 250 UA, 175 KV BEAM.	23
FIGURE 2.6.11: HARMONIC CAVITY SIGNALS FOR A 500 UA, 175 KV BEAM.	24
FIGURE 2.6.12: HARMONIC CAVITY SIGNALS FOR A 500 UA, 175 KV BEAM.	24
FIGURE 3.1.1: A 1497 MHZ HARMONIC CAVITY WITHIN A 10" CONFLAT FLANGE.	26
FIGURE 3.3.1: MEASURED WAVEFORMS FROM A SUCCESSIVELY TRIMMED 499 MHZ BEAM.	28
FIGURE 3.3.2: WAVEFORMS OF SUCCESSIVELY TRIMMED 499 MHZ BUNCH STREAM PROCESSED WITH AN ESTIMATE OF THE HARMONIC CAVITY'S TRANSFER FUNCTION.	28
FIGURE 3.5.1: BUNCH SHAPE MEASURED BY THE DEFLECTION TECHNIQUE OF A 499 MHZ BEAM.	29

FIGURE 3.6.1: HARMONIC CAVITY MEASUREMENTS OF THE 499 MHZ BEAM PROCESSED WITH AN ESTIMATE OF THE CAVITY'S TRANSFER FUNCTION.	30
FIGURE 3.7.1: DEFLECTION MEASUREMENTS OF THE 249.5 MHZ BEAM.	31
FIGURE 3.8.1: HARMONIC CAVITY MEASUREMENTS OF THE 249.5 MHZ BEAM.	32
FIGURE 3.9.1: TWO INTERLEAVED 499 MHZ BEAMS ABOUT 40° OUT OF PHASE.	34
FIGURE 3.9.2: PROCESSED WAVEFORM IS NEARLY 120° FROM BUNCH COINCIDENCE.	34
FIGURE 3.9.3: TWO INTERLEAVED 499 MHZ BEAMS ABOUT 30° OUT OF PHASE.	35
FIGURE 3.9.4: PROCESSED WAVEFORM IS NEAR 90° FROM BUNCH COINCIDENCE.	35
FIGURE 3.9.5: TWO INTERLEAVED 499 MHZ BEAMS ABOUT 20° OUT OF PHASE.	36
FIGURE 3.9.6: PROCESSED WAVEFORM IS NEAR 60° FROM BUNCH COINCIDENCE.	36
FIGURE 3.9.7: TWO INTERLEAVED 499 MHZ BEAMS ABOUT 10° OUT OF PHASE.	37
FIGURE 3.9.8: PROCESSED WAVEFORM NEAR 30° FROM BUNCH COINCIDENCE.	37
FIGURE 3.9.9: TWO INTERLEAVED 499 MHZ BEAMS IN PHASE.	38
FIGURE 3.9.10: PROCESSED WAVEFORM AT BUNCH COINCIDENCE.	38
FIGURE 3.10.1: DC VOLTAGE VS. RELATIVE PHASE OF TWO 499 MHZ BEAMS.	39
FIGURE 3.11.1: THE DETECTED WAVEFORM FROM A 500 KV, 499 MHZ BEAM.	41
FIGURE 3.11.2: THE RELATIVE MAGNITUDE OF THE HARMONIC CAVITY'S RESONANCES.	42
FIGURE 4.1.1: A HYPOTHETICAL 499 MHZ BEAM WITH A 2004 PS PERIOD.	44

FIGURE 4.1.2: THE IFT OF EVERY THIRD TERM OF WAVEFORM OF FIGURE 4.1.1'S
DFT.

44

CHAPTER 1: INTRODUCTION

A resonant cavity was designed to have multiple harmonic TM_{0N0} modes and was used to accurately measure the longitudinal charge profile of a bunched particle beam passing through its bore, non-invasively and in real time. This dissertation will describe the design and development of these cavities as well as measurements made with them.

History: In 1979, a beam bunching cavity was developed at Los Alamos National Laboratory that simultaneously superimposed two harmonic modes, the TM_{010} and TM_{020} modes [3]. This effort was enabled by the development of a breakthrough technology at that time, the RF field solver Poisson/Superfish [4]. By changing the cavity shape in software and solving for the resonance frequencies of these two modes, Scriber and Swenson were able to design a double-frequency TM_{0N0} harmonic cavity before machining metal.

The work presented here is an extension of their efforts and has resulted in cavity designs that superimpose multitudes of TM_{0N0} harmonic modes while suppressing non-axially symmetric modes. Beamline compatible prototypes were developed during this effort and have been installed in several locations at the Thomas Jefferson National Accelerator Facility and have been used to measure the longitudinal profile of electron bunches moving through their bore by determining the relationship between the beams Fourier series and the harmonic resonances induced in the cavity.

Other notable non- TM_{0N0} harmonic cavity projects, present and past, can be found in references [5,6].

1.1 Multi-harmonic TM_{0N0} cavities

Multi-harmonic TM_{0N0} cavities, referred to throughout this dissertation as harmonic cavities, have been designed to simultaneously resonate many harmonic TM_{0N0} modes, and to suppress or displace TE and non-axially symmetric TM modes. A cavity with many harmonic TM_{0N0} modes, and having a mode spectrum free of interfering resonances, can be used for harmonic mode superposition.

Harmonic mode superposition can be visualized in Figure 1.1.1, which shows four TM modes in a cylindrical cavity. The TM_{010} , TM_{020} , TM_{030} , and TM_{040} modes are presented below. The figure represents the instantaneous electric field superposition of these modes if simultaneously driven in the same cavity.

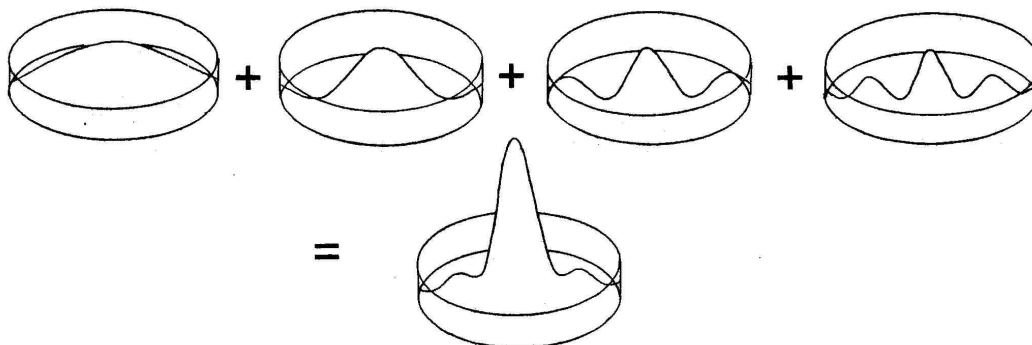


Figure 1.1.1: An illustration of the superposition of the TM_{010} , TM_{020} , TM_{030} , and TM_{040} resonant modes at a moment of simultaneous electric field maximum.

One reason to develop multi-harmonic TM_{0N0} cavity designs is because the electric fields of these modes are additive; the superimposed electric field on-axis is four times greater than the field of a single mode alone. Achieving a four-fold increase in the electric field by increasing input power into a single mode would require four times the

RF power. This is because the field intensity in a resonant cavity is proportional to the square root of its input power.

Another reason to pursue the development of multi-harmonic TM_{0N0} cavity designs is because the electric field maximum of these modes is along the cavity's axis of symmetry and bore, allowing the cavity's multiple resonances to interact with a beam of charged particles passing through it.

A pillbox cavity, a hollow metal cylindrical shell, is a common RF resonator example found in textbooks because its resonant modes can be solved analytically. The mode spectrum of a pillbox cavity is a chaotic mix-up of non-harmonic TM_{0N0} modes interspersed with transverse resonant modes. RF field solvers, like Superfish, provide cavity designers the ability to solve mode geometries that would be impossible to solve analytically, and to manipulate their geometry so that high order modes can be made to be regular and useful.

The mode spectrum of the TM_{0N0} modes in an axially symmetric cavity can be manipulated to becoming harmonic by altering the cavity's geometry, and non TM_{0N0} modes can be suppressed by controlling the conductive paths on the cavity walls, and TE modes can be displaced by lowering the cavity height.

Multi-harmonic cavity shape solutions were found by iteratively modifying an axially symmetric cavity shape with an axial bore, while solving for multiple TM_{0N0} mode frequencies with the field solver POISSON/Superfish.

A continuous family of geometric solutions was the result; five are shown in Figure 1.1.2.

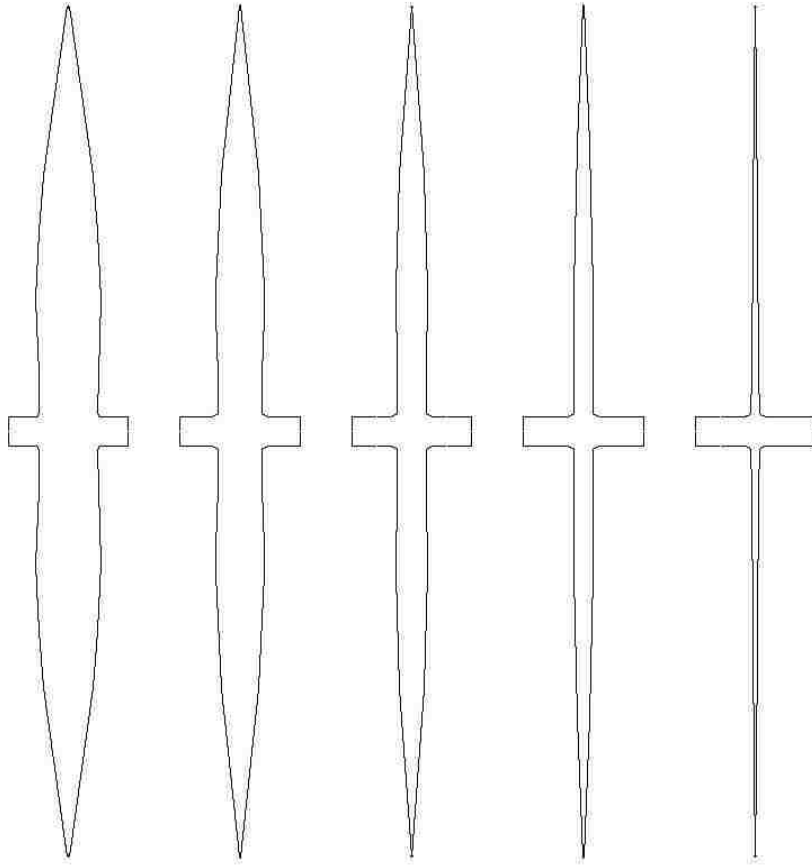


Figure 1.1.2: Some of the cavity geometries that have harmonic TM_{0N0} modes are shown in cross section with a horizontal axis of symmetry and beam tube.

The shallowest saucer shaped cavities of Figure 1.1.2 (right side) has a mode spectrum that is clear of TE modes for many octaves because TE modes resonate at frequencies greater than $c/2h$ where h is the cavity length along the beam's direction of motion [7]. The wider geometries (left side) have higher Q's because cavity Q is proportional to the cavity's ratio of volume to surface area [8]. Electric field solutions for harmonic TM_{010} - TM_{080} modes, as solved for by Superfish for the center geometry shown in Figure 1.1.2, are shown in Figure 1.1.3 in cross section with the beam tube horizontal.

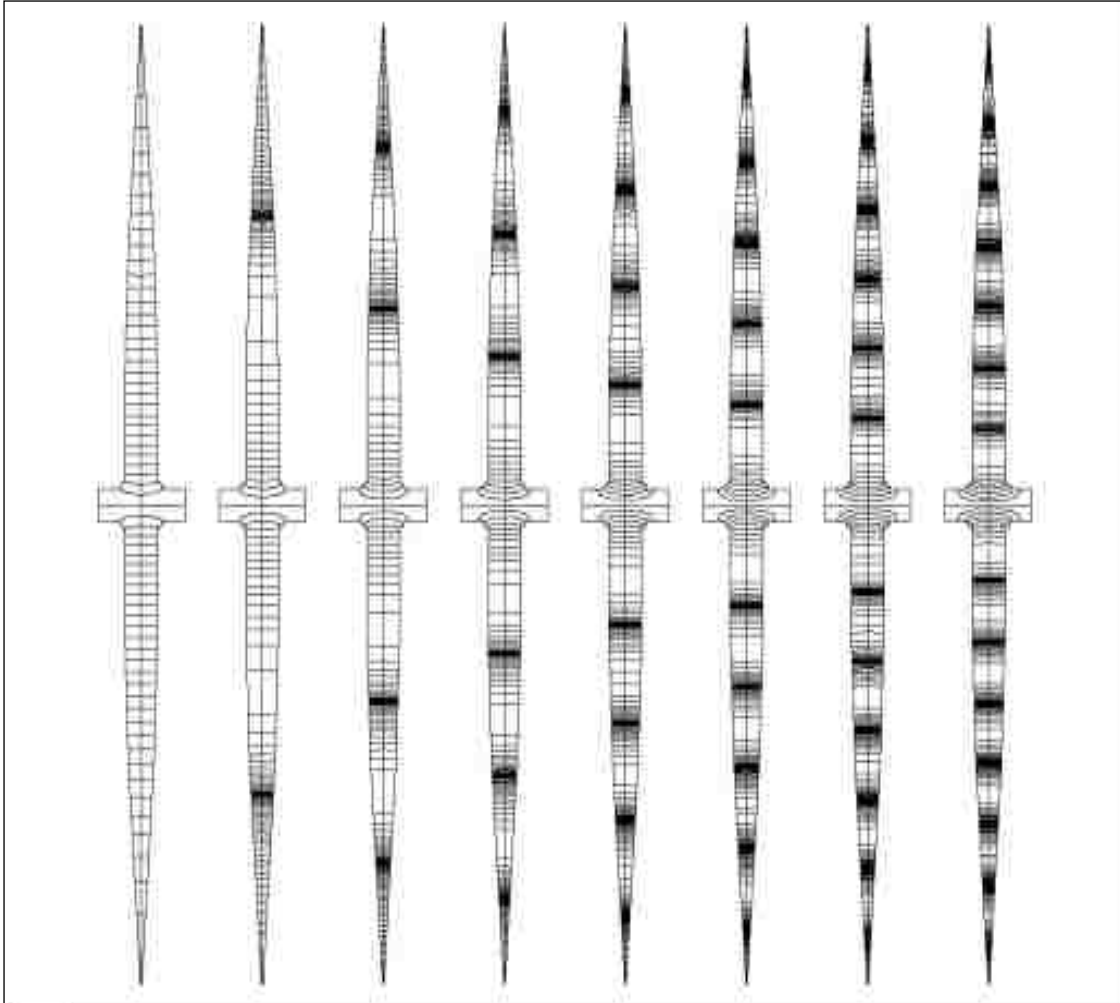


Figure 1.1.3: Electric field solutions for the TM_{010} - TM_{080} modes.

The time evolution of the superposition of harmonic TM_{010} - TM_{080} modes driven simultaneously is shown in Fig. 1.1.4. Rolling your eyes around these images show one cycle of the fundamental frequency of the harmonic cavity.

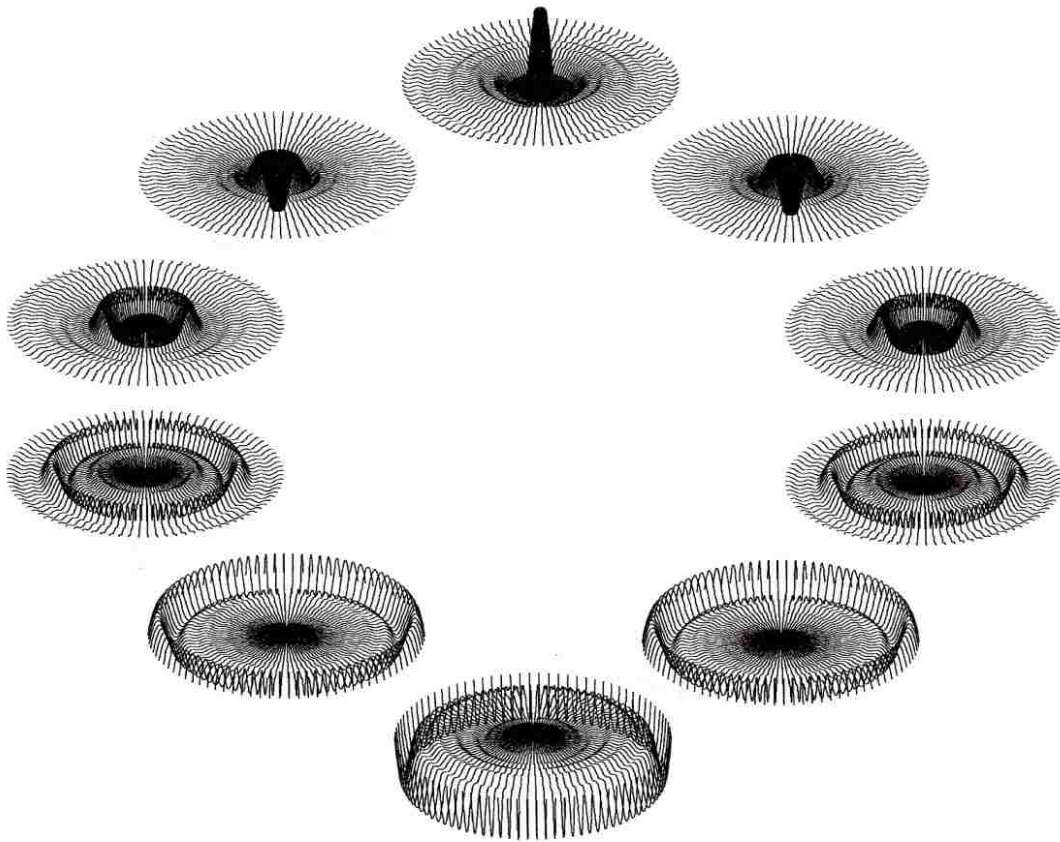


Figure 1.1.4: The time evolution of the superimposed modes TM_{010} - TM_{080} for the cavity in Figure 1.1.3 with its axis of symmetry oriented vertically.

The superposition of multiple harmonic TM_{0N0} modes can be similar to the waves generated in a coffee cup by dropping in a cube of sugar.

A beam line-compatible harmonic cavity was machined from aluminum in two halves, welded together, and installed within a 12" Conflat vacuum flange. A harmonic cavity shape was cut into these two halves using a CNC milling machine and a ball shaped end mill that cut radially following a profile shown in Figure 1.1.2. To inhibit non-axially symmetric TM modes in the prototypes, radial slits were machined into the

cavity walls that suppress non-radial wall currents. In Figure 1.1.5 these slits can be seen. Wide slits were cut from the back, followed by a thin slits that penetrate through the cavity's inner surface.



Figure 1.1.5: A beamline compatible harmonic cavity constructed for testing on the Jlab Injector Test Facility.

The TM_{0N0} modes have purely radial wall currents and are unaffected by these slits, while the TM_{MNP} modes with azimuthal mode numbers (m) less than the number of discontinuities cannot resonate. A single wideband loop antenna connected to the center pin of the SMA connector on the bottom of Figure 1.1.6 traverses the cavity along its plane of symmetry and bends 90° near the bore and connects to the cavity wall, coupling to all of the cavity's harmonic TM modes.



Figure 1.1.6: The cavity of Figure 1.1.5 sandwiched between two 12" to 2 $\frac{3}{4}$ " flange reducers to make it compatible with Jlab's Injector Test Facility beamline.

This dissertation summarizes the work performed under the auspices of DOE SBIR Phase I and II grant DE-SC0009509 to develop a noninvasive electron beam bunchwidth diagnostic. The remainder of this dissertation is organized as follows. Chapter 2 presents measurement results at the Injector Test Facility at Jlab. Chapter 3 presents measurement results at CEBAF of a 499 MHz beam, a 249.5 MHz beam, and compares them to measurements made simultaneously by the deflection technique. It also presents measurements of interleaved 499 MHz beams detected by a sampling oscilloscope as well as by an RF detector and voltmeter. The harmonic cavity's response to a 500 kV beams is also described. Chapter 4 presents a review of subharmonic measurements, a review of key concepts, a conclusion, and

recommendations for future work. Finally, the Appendices contain additional supportive information.

CHAPTER 2: MEASUREMENTS AT THE INJECTOR TEST FACILITY

2.1: The Injector Test Facility (ITF)

The ITF is a DC photogun and experimental beamline. A photogun uses pulsed laser light to liberate electrons from the surface of a solid cathode material by the photoelectric effect. At the Jefferson lab, the cathode of choice is crystalline Gallium Arsenide (GaAs) because it can liberate spin polarized electrons that are useful for Nuclear Physics experiments. The cathode is biased to a high voltage in a Pierce configuration [9], so that the liberated electrons are quickly accelerated, focused, and sent down the experimental beamline.

The photogun laser is a gain switched diode [10] followed by fiber amplifiers and in some cases frequency doubling crystals to produce 35 ps FWHM Gaussian shaped pulses of light. Ideally, the pulsed laser ejects photoelectrons from the cathode's surface, and the longitudinal profile of the electron bunches leaving the cathode is the same Gaussian shape as the laser's pulses. In practice, some of the laser light penetrates through the surface of the cathode material and subsurface electrons are also emitted. The subsurface electrons can leave the cathode after the laser pulse terminates because they have further to travel, and because they interact with the GaAs crystal lattice as they exit. This effect can produce an unwanted tail on the electron bunches. As the electron bunches propagate down the beamline, space charge forces within them cause them to expand.

In general, the higher the accelerating voltage, and the lower the beam current and bunch charge, the closer the bunch shape resembles the Gaussian laser pulse shape that generated it.

A technique to reduce the electron bunch's unwanted tail is to use a GaAs superlattice rather than a bulk GaAs photocathode. GaAs superlattice cathodes consist of multilayers of crystalline GaAs interleaved with dopants to concentrate the laser's interaction to the surface. Superlattice cathodes can be constructed with integrated Bragg reflectors [11] to decrease the laser's penetration into the material.

The ITF photogun has adjustable accelerating voltage, adjustable laser pulse repetition rate, and a load-locked photocathode, so that different cathode materials can be efficiently tested.

2.2 Harmonic cavity testing on the ITF beamline

The harmonic cavity in Figures 1.1.5 and 1.1.6 was installed on the ITF experimental beamline 5 meters from the gun so that the beam passed through its bore. A sampling oscilloscope was connected to the harmonic cavity's output antenna through a low loss coaxial cable.

The load-lock on the ITF photogun allowed the staff of Jlab's Center for Injectors and Sources (CIS) to easily exchange the cathode material. 1533 MHz beams of three currents (25 μ A, 250 μ A, and 500 μ A), two different accelerating voltages (75 kV and 175 kV), and two different cathodes (bulk GaAs and superlattice) were transmitted through the harmonic cavity. Full wavelength waveforms were captured from the sampling oscilloscope for each of these parameters and cathodes.

The sharpest detected response was induced by the lowest current (27 μA), highest voltage (175 kV), beam emitted by a superlattice photocathode; a complete wavelength of the periodic signal is shown in Figure 2.1.1.

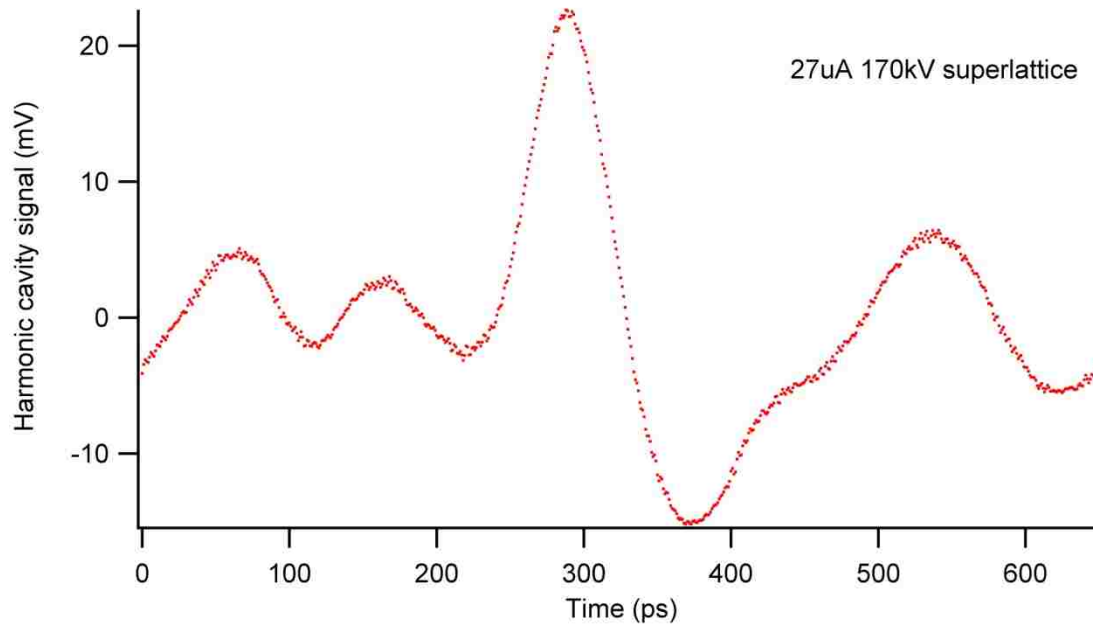


Figure 2.2.1: One wavelength of the harmonic cavity's response to a 27 μA , 175 kV, 1533 MHz beam created using a superlattice photocathode.

As the bunched beam passes through the harmonic cavity at its fundamental frequency (1533 MHz), many $\text{TM}_{0\text{N}0}$ modes are induced to resonate; the detected waveform is the superposition of these excited modes.

Key Concept #1: The waveform exported from the cavity's antenna and detected by the oscilloscope is the superposition of the cavity's resonant modes excited by the beam and coupled out of the cavity.

2.3: The Discrete Fourier Transform (DFT) and the harmonic cavity's mode by mode response

The output of a sampling oscilloscope consists of discrete points that are evenly separated in time. The Discrete Fourier Transform (DFT) of an even number of points (N) of one complete wavelength of a periodic signal produces $N/2$ complex [12] terms that are the signal's positive frequency components. These complex terms represent the waveform's DC offset, the relative phase and amplitude of each individual cavity resonance detected by the oscilloscope, and noise on the signal.

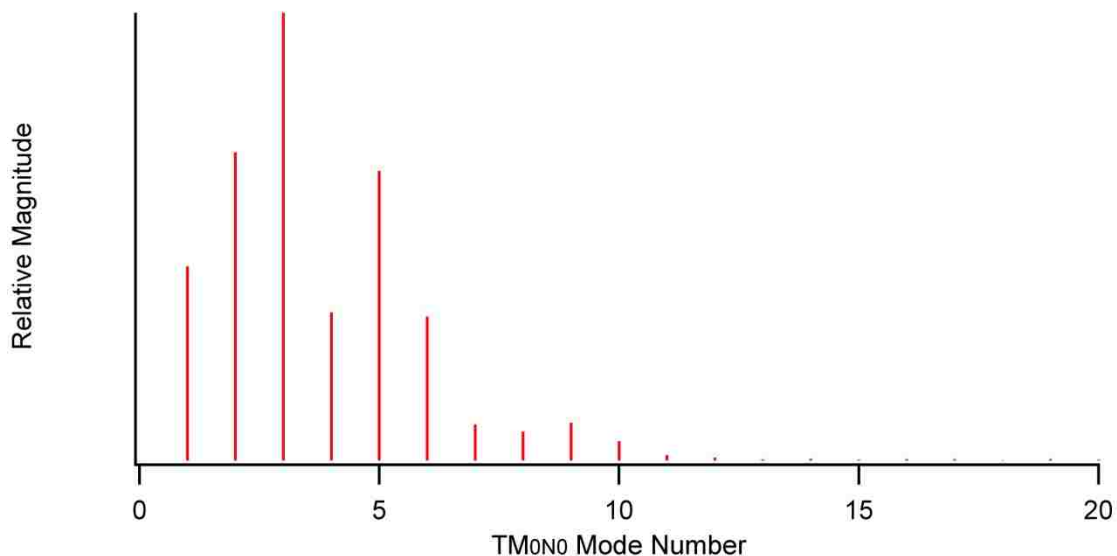


Figure 2.3.1: A graph of the relative magnitude of the harmonic cavity resonances excited by the beam and coupled to the oscilloscope showing the first 20 of $N/2$ positive frequency terms.

The first term in a DFT represents the DC offset and is only nonzero if the oscilloscope's trace is offset. Figure 2.3.1 shows the magnitude of these complex numbers to show the contribution of each cavity mode, as would be seen by a spectrum

analyzer connected to the cavity's antenna. This graph is terminated after the 20th term/mode rather than $N/2$ to highlight the contribution of each cavity resonance. The beam in this example has excited the $TM_{010} - TM_{0,10,0}$ modes in the harmonic cavity to resonate. The small terms beyond these represent noise on the measured signal.

Key Concept #2: The relative amplitude and phase of each individual harmonic cavity mode, as it is coupled out of the cavity, can be determined from the detected waveform by calculating the waveform's DFT of one wavelength of the signal.

2.4 Distortion in the harmonic cavity signal

Distortion in the measured signal is caused by at least three sources: harmonic cavity imperfections, non-uniform antenna coupling, and cable dispersion.

Harmonic cavity imperfections are misalignments between the frequency of the resonant modes in the harmonic cavity and the harmonics of the bunch frequency. A mode driven on the shoulder of its resonance curve causes a decrease in detected amplitude as well as a phase shift between the beam and the excited mode, a concept embodied the universal resonance curve [12].

The antenna's coupling and uniformity is also a source of distortion. The single loop antenna is ideally a magnetic field loop that responds out of phase from the electric field of each resonance. The loop antenna is also influenced by the electric field of the resonances because it loops to ground parallel to this field. The phase shift induced by the antenna is the combined influence of these fields and is mode-dependent. The single antenna does not couple uniformly to all of the modes in the cavity. This causes

amplitude differences between the excited resonances and their contribution to the detected waveform.

Coaxial cables cause distortion by dispersion and frequency-dependent losses. Dispersion is frequency-dependent propagation velocity that causes an induced phase shift that increases with frequency. Attenuation in coaxial cables is frequency-dependent and higher frequencies are more strongly attenuated.

Key Concept #3: Distortion in the detected waveform is caused by an imperfect antenna, an imperfect harmonic cavity, and cable dispersion.

Despite the complexity of these sources of distortion, their combined effect is simply a mode by mode, or term by term phase shift and amplitude difference between what is induced and what is detected. All that is needed to correct for the combined distortion is a single complex term per mode that, when multiplied by the corresponding term of its detected waveform DFT, properly scales its amplitude and shifts its phase. The series that corrects for these combined sources of distortion is the harmonic cavity's transfer function.

Key Concept #4: The harmonic cavity's transfer function can be used to correct distortion.

2.5 An estimate of the harmonic cavity's transfer function

The harmonic cavity's transfer function is the ratio of two Fourier series, the DFT of a brief detected waveform and the DFT of the electron bunch shape that induced it. When multiplied with the DFT of subsequent measurements, the inverse transform

produces an undistorted signal. Each term of the transfer function properly scales the magnitude and shifts the phase of each detected harmonic cavity resonance to remove the effects of distortion.

Key Concept #5: The harmonic cavity's transfer function is the ratio of two Fourier series, one is the DFT of a brief detected waveform, and the other is the Discrete Fourier series of the true beam current.

While the bunch shape of the beam that induced the detected waveform is not precisely known, it can be searched for and found by the technique of blind deconvolution [13,14]. Using this technique, prototype transfer functions are tested and iterated based on what is precisely known about the inducing beam, that between bunches, the measured waveform should be flat.

The procedure used for processing waveforms:

- 1) Select a harmonic cavity signal from a low current, high energy beam and trim it to an even number of points that compose one complete wavelength. Fit a Gaussian with the same number of points to the most prominent feature of the detected waveform.
- 2) Calculate the complex DFT of both waveforms and divide the detected DFT into the Gaussian DFT. This is a prototype inverse transfer function.
- 3) Apply this transfer function by multiplying it with the DFT of subsequent measurements and calculate the products IFT for evaluation.
- 4) Increase the FWHM of the Gaussian and interpolate to the same number of points and repeat until the results have flat baseline.

The inverse transfer function is calculated to prevent divide by zero errors. A perfect Gaussian has no signal noise, so its high order harmonics are all zero. Division into these terms removes measurement noise from the processed waveforms.

The prototype inverse transfer function is then tested by multiplying it with the complex DFT of subsequent measurements that are trimmed to one wavelength and have the same number of points. The inverse transform of this product produces modified waveforms for evaluation.

Transfer functions created using a Gaussian fit of a detected signal typically result in processed waveforms with significant ripples on the baseline. This can be resolved by incrementally widening the Gaussian by trimming points from the front and back of the waveform and using point interpolation to return the estimate to the same number of points and calculating a new transfer function. The transfer function that produces a flat baseline also produces the best approximation of true bunch shape.

The waveforms processed from this procedure are only approximations of the true wave shape because the procedure relies on the assumption that a brief, low current bunch profile has a perfect Gaussian bunch shape. What is required to find the true bunch shape is an automated algorithm that can increment the assumed bunch shape and solve for a flat baseline in processed waveforms.

Key Concept #6: The harmonic cavity's transfer function can be estimated, tested, and refined by the method of blind deconvolution.

Figure 2.5.1 shows the Gaussian wave shape that was used with the waveform in Figure 2.2.1 to create a transfer function that processed measurements from the

experiments described below.

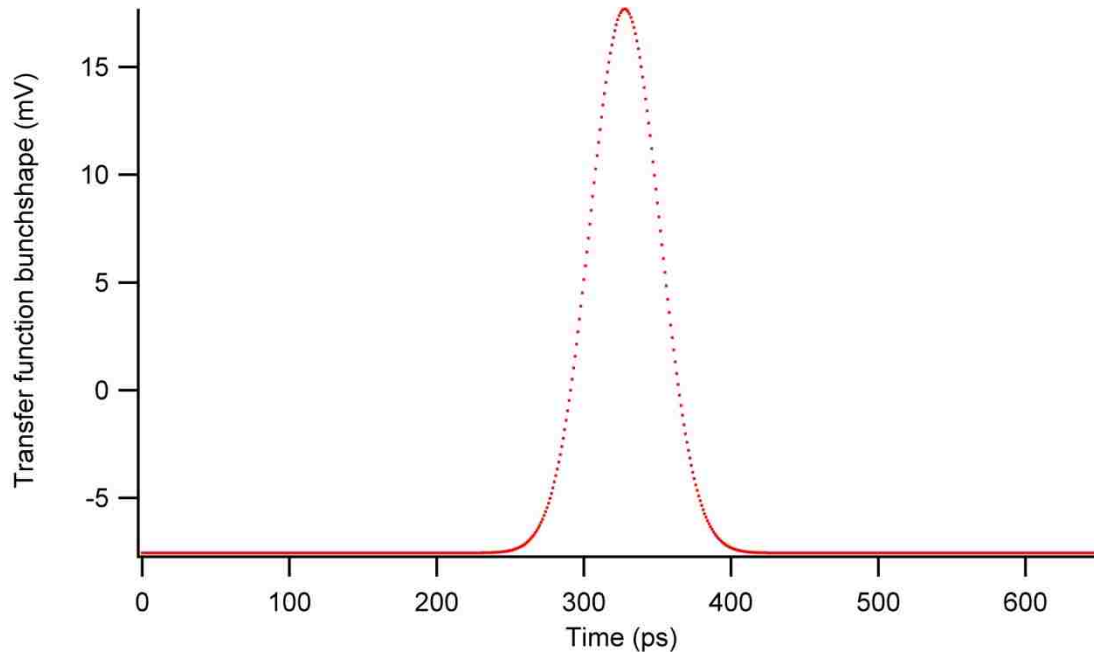


Figure 2.5.1: An estimate of a 25 μA and 175 kV beam's longitudinal profile.

1533 MHz beams were created using two different cathodes: bulk GaAs and superlattice and transmitted through the harmonic cavity. Three different beam currents 25 μA , 250 μA , and 500 μA were accelerated at two different voltages of 75 kV and 175 kV and measured. Figures 2.6.1-2.6.12 show the detected and processed waveforms from this set of experiments, the first three at 75 kV where space charge forces have significant effect on the bunch shape, and the second three at 175 kV. The plots are viewed with the head of the bunch on the left and the tail of the bunch on the right. The tail from the bulk GaAs cathode can be seen in the blue traces.

2.6 Measurements of Bulk GaAs and superlattice at 75 kV and 175 kV accelerating voltages

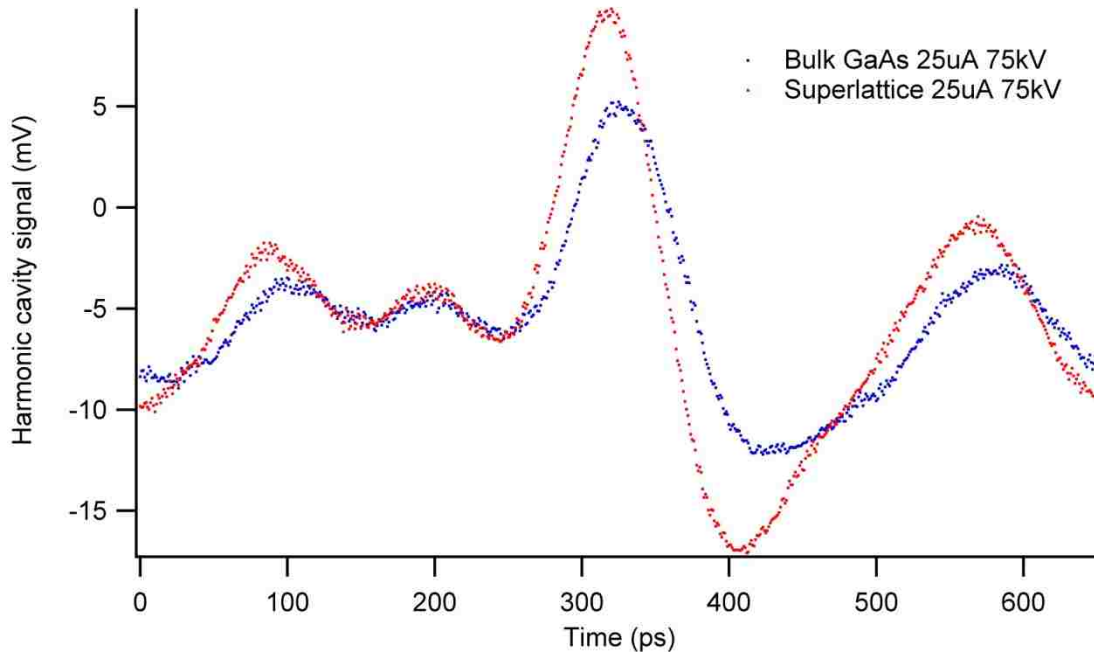


Figure 2.6.1: Harmonic cavity signals for a 25 uA, 75 kV beam.

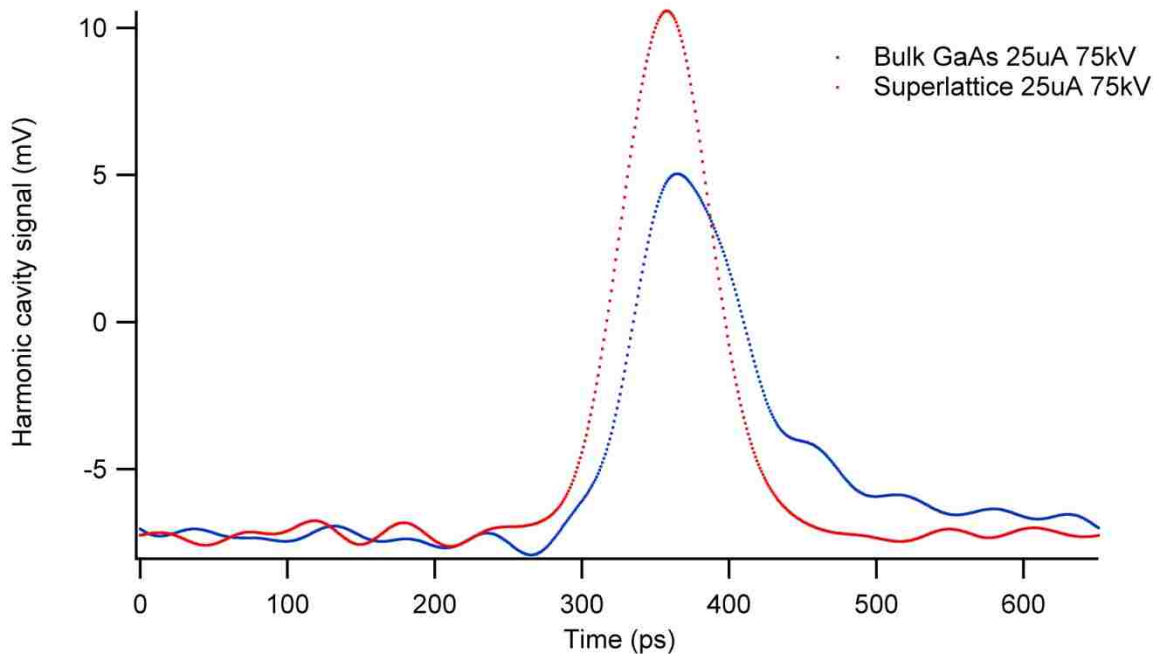


Figure 2.6.2: Processed signals for a 25 uA, 75 kV beam.

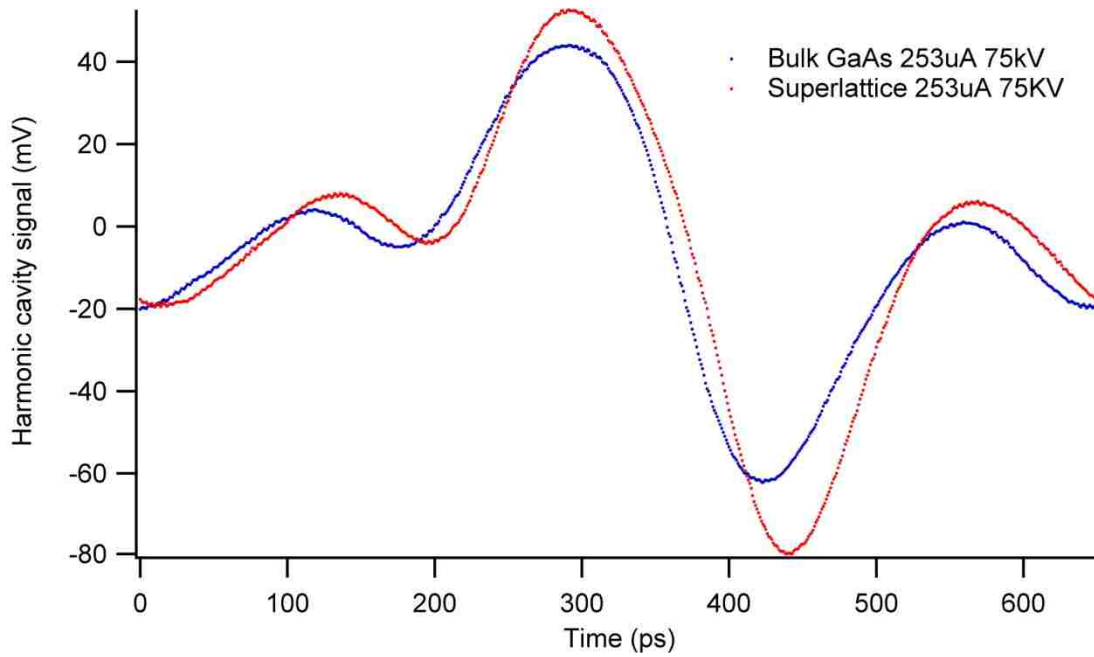


Figure 2.6.3: Harmonic cavity signals for a 250 uA, 75 kV beam.

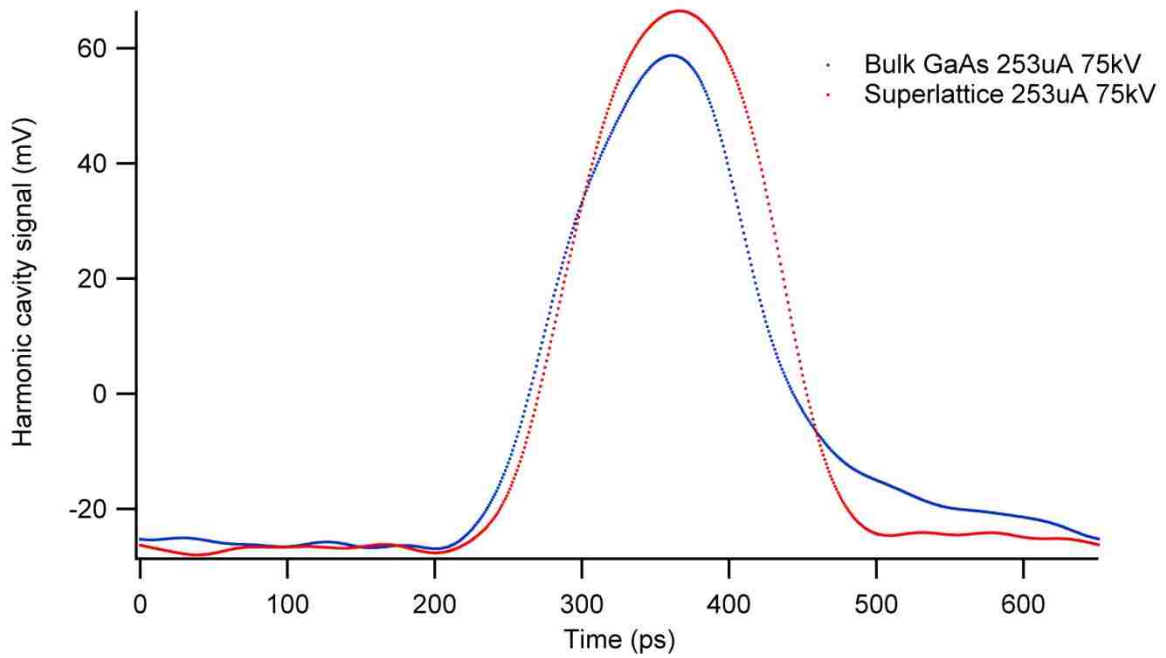


Figure 2.6.4: Processed signals for a 250 uA, 75 kV beam.

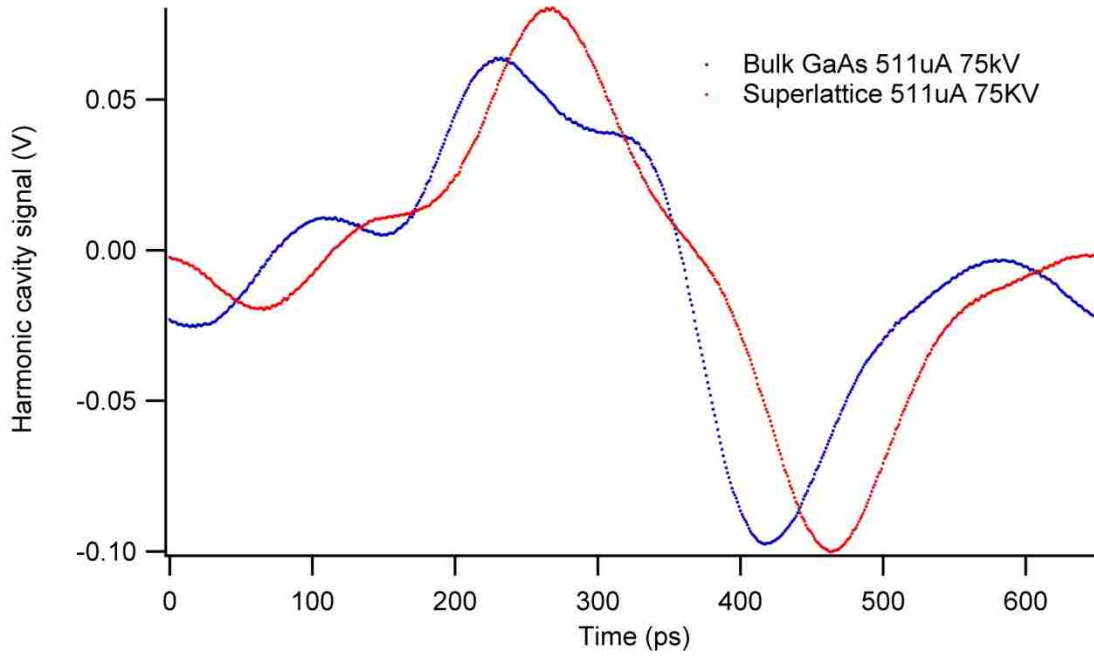


Figure 2.6.5: Harmonic cavity signals for a 500 uA, 75 kV beam.

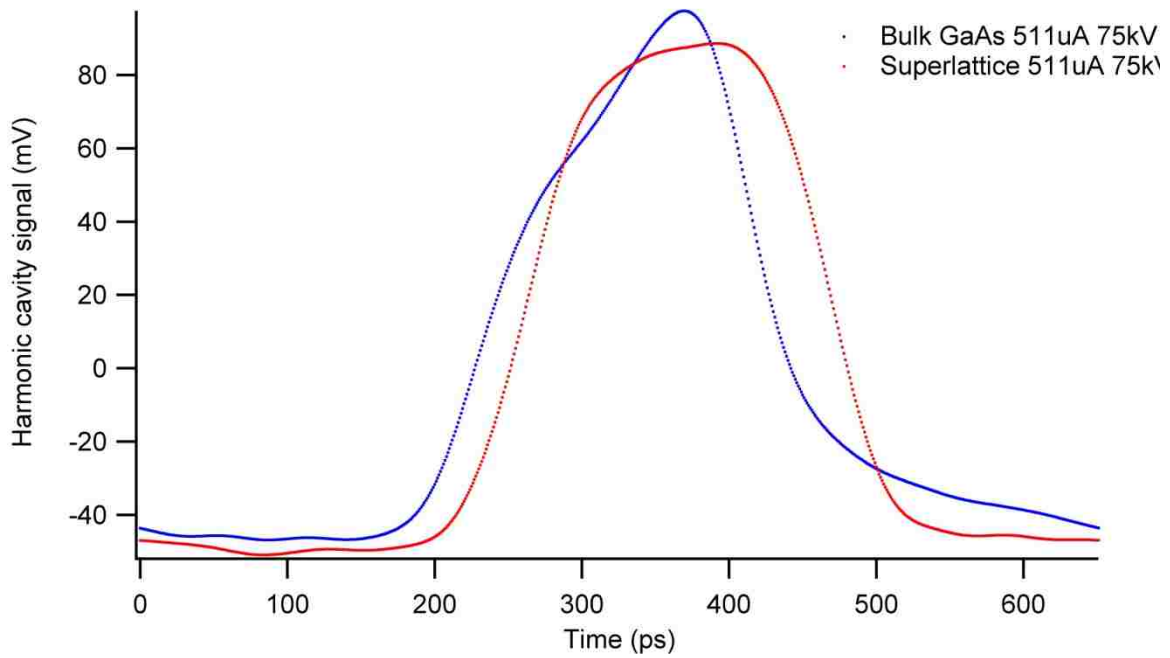


Figure 2.6.6: Processed signals for a 500 uA, 75 kV beam.

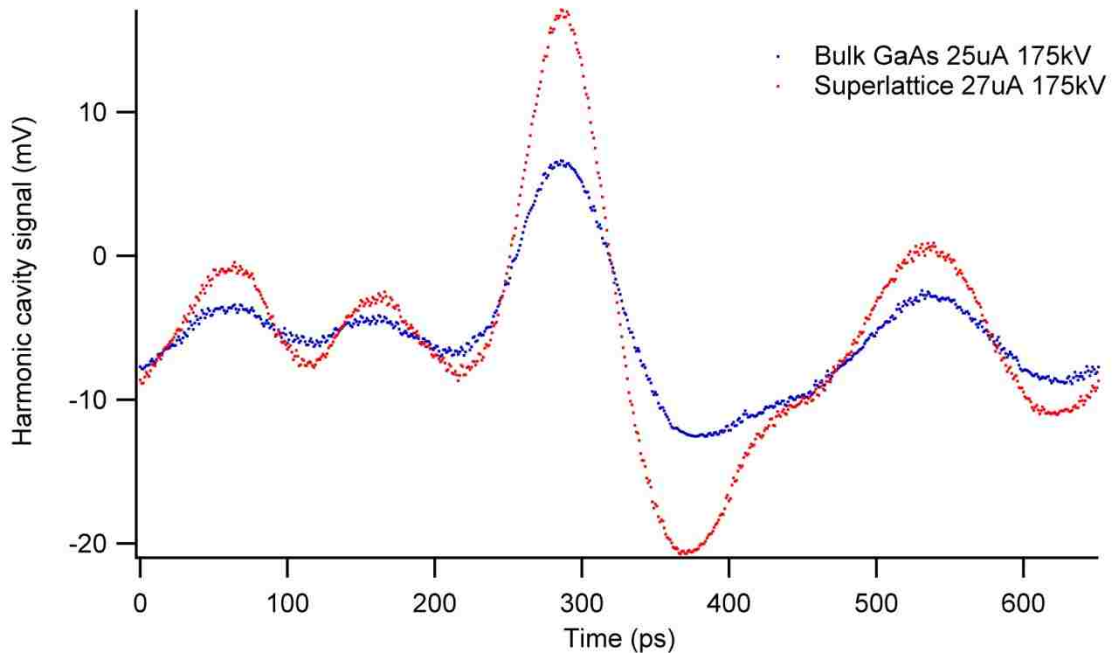


Figure 2.6.7: Harmonic cavity signals for a 25 μA , 175 kV beam.

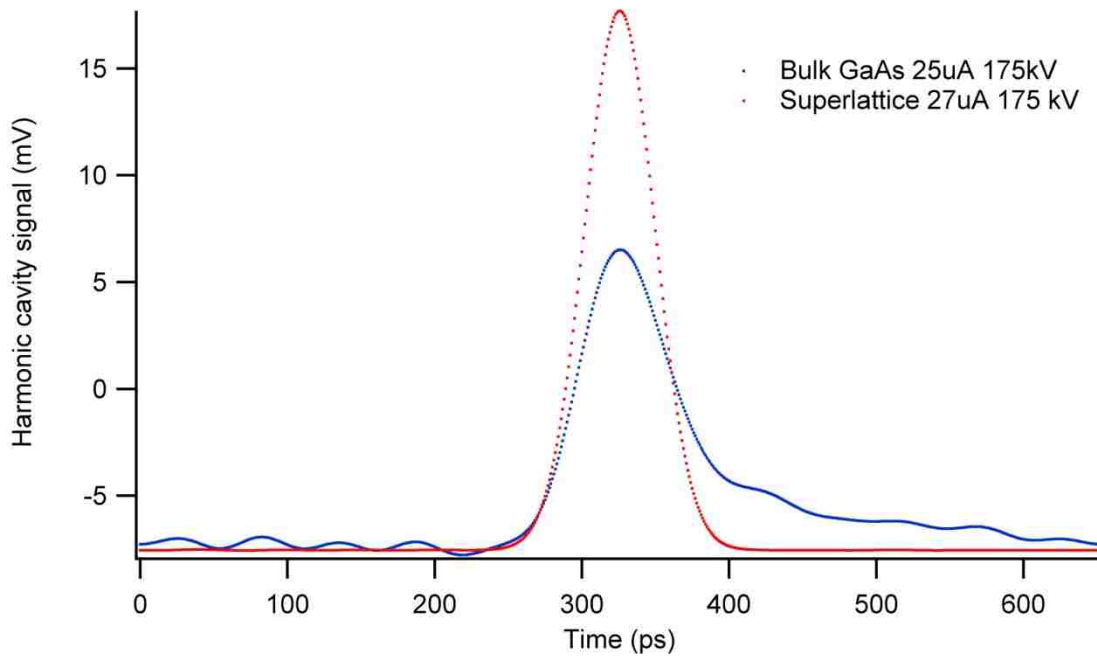


Figure 2.6.8: Processed signals for a 25 μA , 175 kV beam.

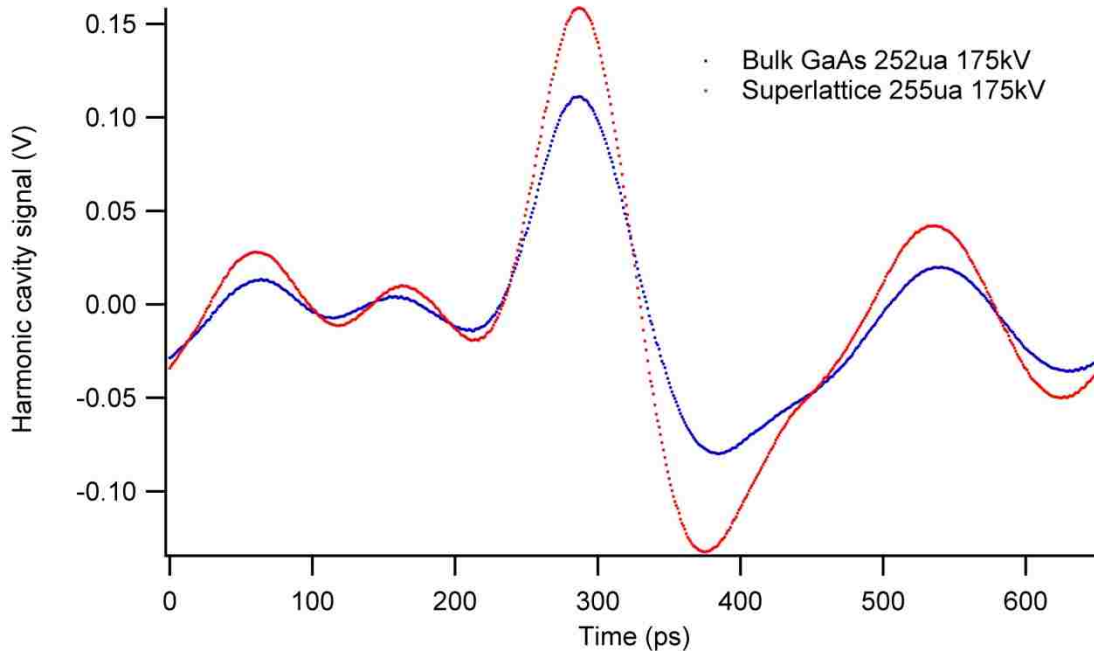


Figure 2.6.9: Harmonic cavity signals for a 250 uA, 175 kV beam.

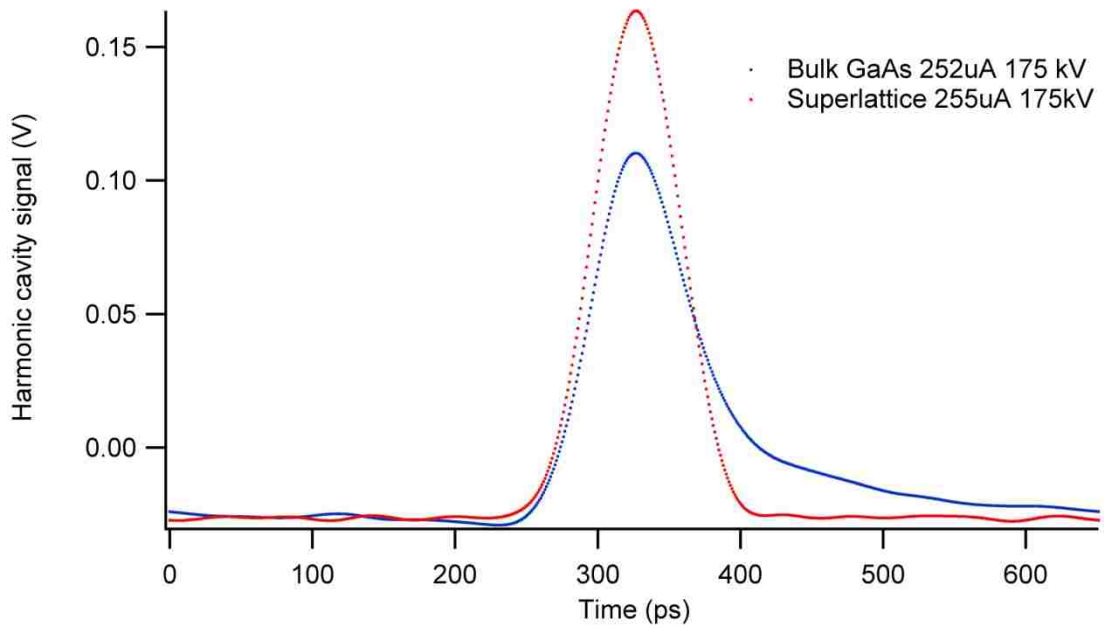


Figure 2.6.10: Processed signals for a 250 uA, 175 kV beam.

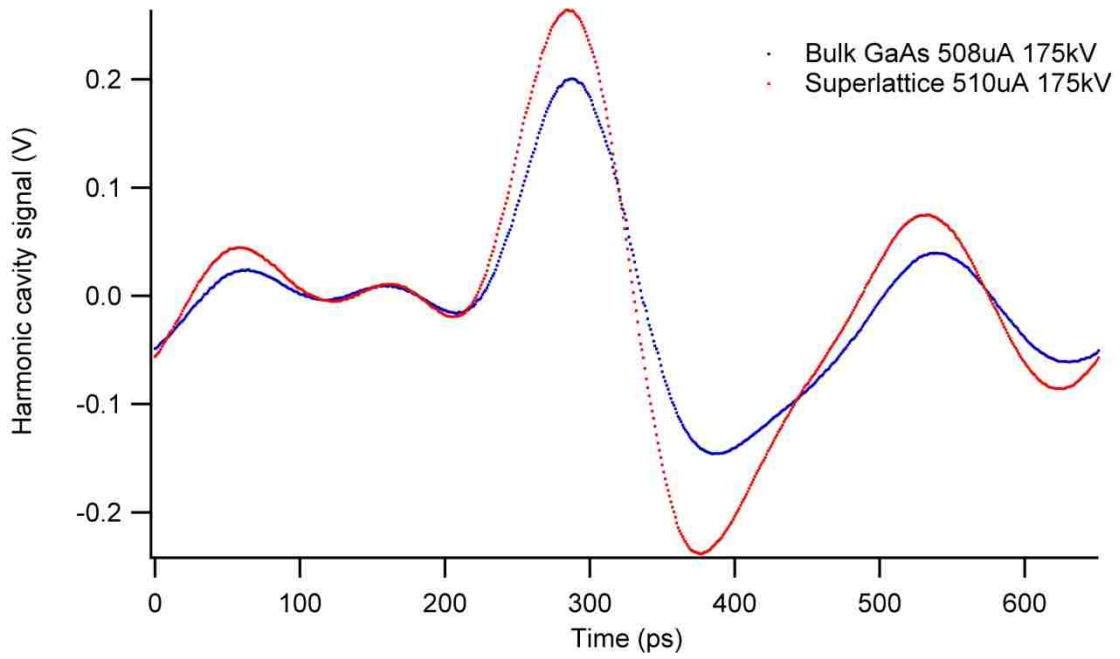


Figure 2.6.11: Harmonic cavity signals for a 500 uA, 175 kV beam.

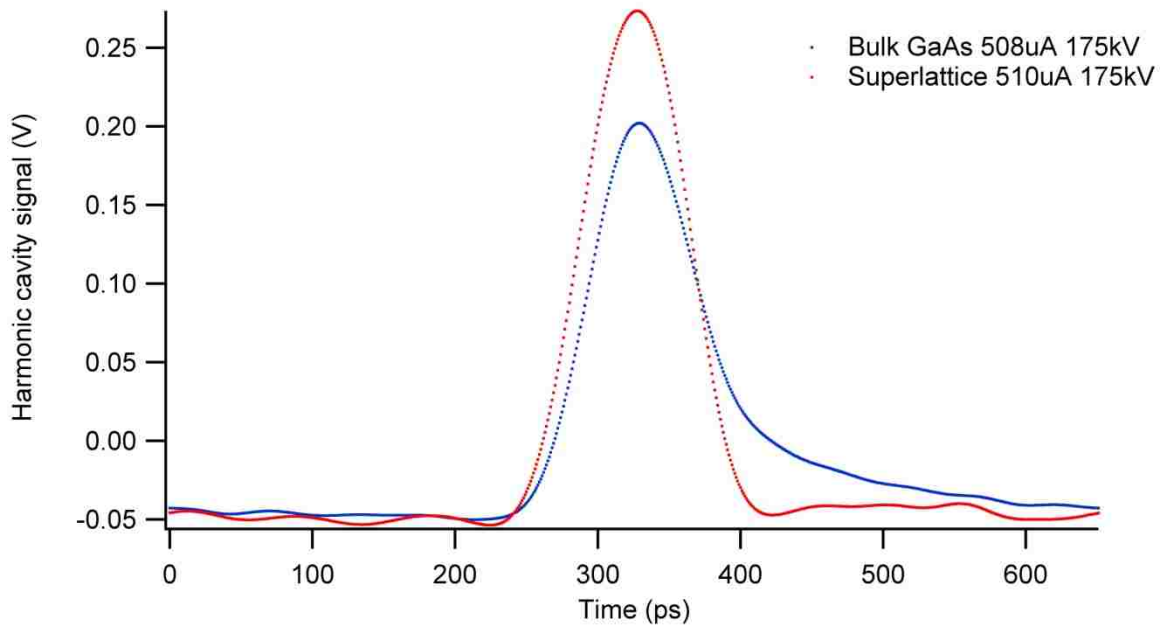


Figure 2.6.12: Harmonic cavity signals for a 500 uA, 175 kV beam.

Figures 2.6.1 through 2.6.12 show how a simple estimation of the harmonic cavities transfer function can be used to remove distortion from the detected waveforms. Measurements at 75 kV demonstrate how space-charge induced bunch growth can significantly affect bunch shape, and measurements at 175 kV demonstrate how accelerating voltage can be used to reduce these effects. All of these measurements show the relative performance and tail signatures of the two photocathode types.

CHAPTER 3: MEASUREMENTS AT THE CONTINUOUS ELECTRON BEAM ACCELERATOR FACILITY (CEBAF)

3.1: A 1497 MHz harmonic cavity

A 1497 MHz harmonic cavity was designed within a 10" Conflat flange and was constructed from two bolted together halves that compressed a malleable wire seal and is shown in cross section in Figure 3.1.1.

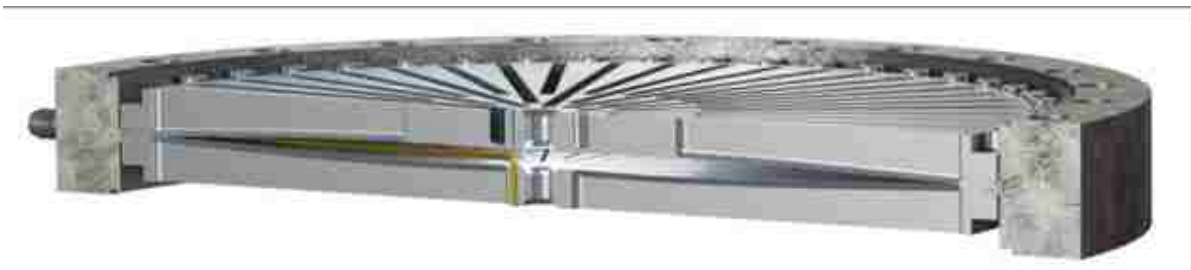


Figure 3.1.1: A 1497 MHz harmonic cavity within a 10" Conflat flange.

3.2 The CEBAF injector

At CEBAF, three independent 499 MHz bunch trains are extracted from a single photocathode inside of a dc 130 kV photogun [4]. These pulse trains are interleaved in time and injected into the accelerator where 1497 MHz superconducting RF cavities increase the beam energy to many GeV. Post acceleration the three beams are un-interleaved and delivered to three experiment halls. The different halls have different beam current requirements, so each beam is created by a different laser operating at 499 MHz.

CEBAF's original electron gun was thermionic and it produced a continuous beam of electrons that was "chopped" into 1497 MHz beam. The chopping system, as it is called, consists of two deflector cavities and a chopping plate. The deflector cavity is a 499 MHz TM_{210} mode cavity driven in two (degenerate) orthogonal transverse deflecting modes, phased to sweep the beam onto a circle on the chopping plate with a revolution frequency of 499 MHz. The chopping plate has three equally spaced holes with adjustable apertures so that three unique bunch streams could be created with the portion of the beam that passes through the apertures. The beam was relinearized with a second identical deflector cavity downstream of the chopping plate.

Now that CEBAF uses a photogun, the chopping system has new uses. It can be used to remove the tail from electron bunches created with the photogun by phasing the beam to pass through the apertures, and then adjusting the phase so that the aperture edge intersects with the tail side of the bunch. It can be used to chop the edge of the bunch to adjust beam current or bunch shape, it can also be used to make precision bunch width and shape measurements.

3.3 Chopping a 499 MHz beam

The 1497 MHz harmonic cavity was installed downstream of the chopping system and an 25 μ A 130 kV, 499 MHz beam was transmitted through it. Measurements were performed as the tail side of the bunch was successively trimmed until there was no transmission through the aperture.

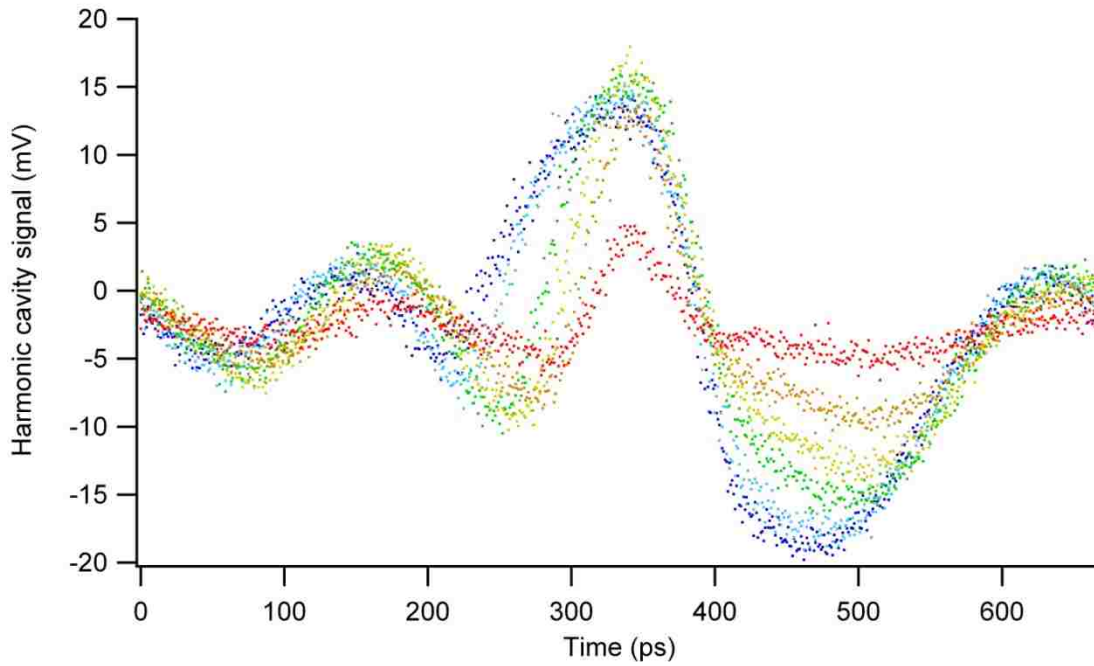


Figure 3.3.1: Measured waveforms from a successively trimmed 499 MHz beam.

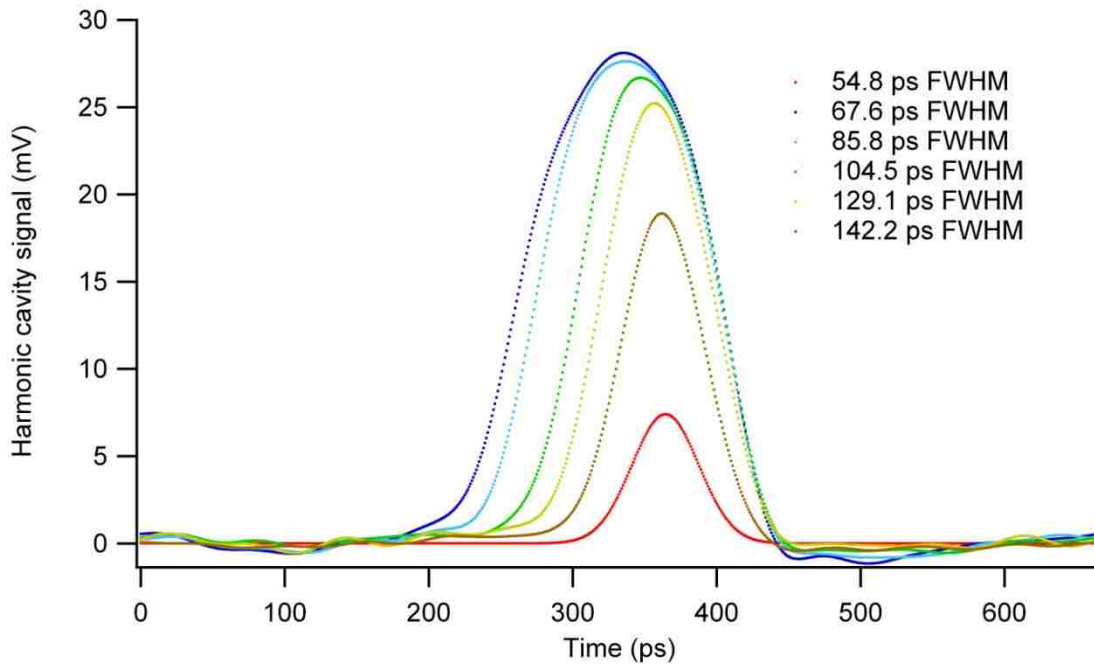


Figure 3.3.2: Waveforms of successively trimmed 499 MHz bunch stream processed with an estimate of the harmonic cavity's transfer function.

3.4 The RF deflection technique

The RF deflection cavity technique of bunch measurement is made by adjusting a chopping aperture to a very thin slit that chops out a thin slice of each bunch. By changing the lasers phase relative to the deflector cavity's, the bunch can be stepped across this slit, and a downbeam Faraday cup measures the current from each slice and produces a slice by slice measurement of bunch profile. Laser 1's pulses are 45 ps FWHM.

3.5: Measurements of the 499 MHz beam by the deflection technique

The bunch shape measured by the deflection technique of a 499 MHz beam is shown in Figure 3.5.1.

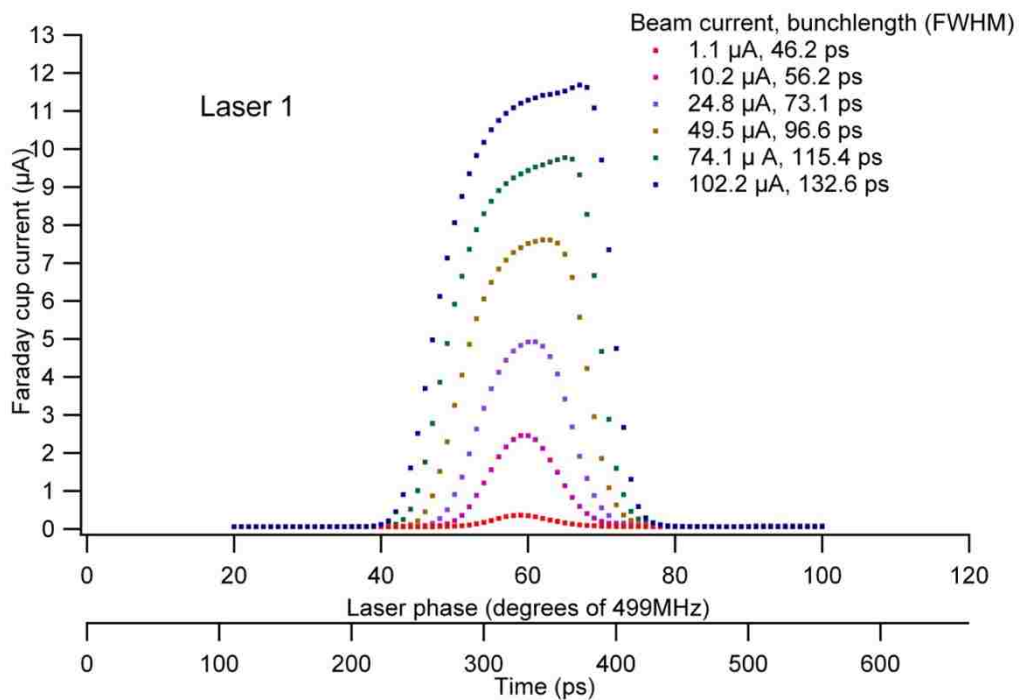


Figure 3.5.1: Bunch shape measured by the deflection technique of a 499 MHz beam.

The deflection technique is a well-established invasive measurement of bunch profile. Each point on the graphs represents the faraday cup current measured for each slice of the bunch stream.

3.6: Measurements of the 499 MHz beam with a harmonic cavity

Figure 3.6.1 presents the results from harmonic cavity measurements of the 499 MHz beam processed with an estimate of the cavity's transfer function.

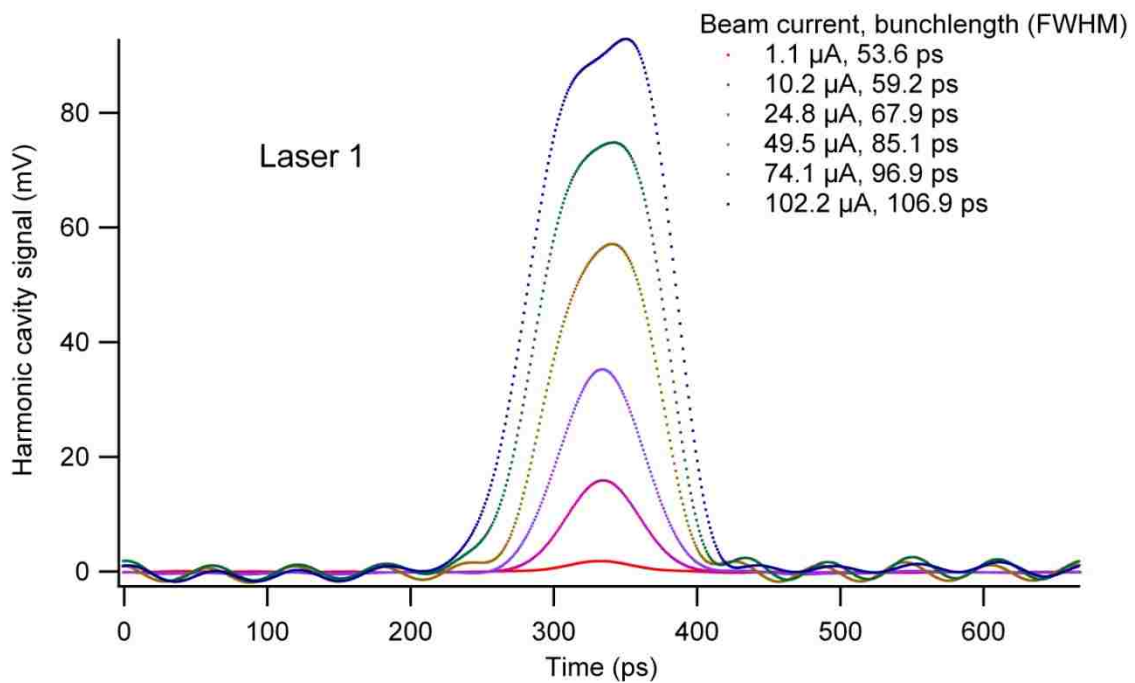


Figure 3.6.1: Harmonic cavity measurements of the 499 MHz beam processed with an estimate of the cavity's transfer function.

During these measurements the harmonic cavity was installed on CEBAF between the gun and the chopping system. Bunch growth between the harmonic cavity

and the chopping system, where the deflection measurements were made, was modeled and corroborated with ASTRA [15] in [2].

3.7: Measurements of the 249.5 MHz beam by the deflection technique

Figure 3.7.1 presents the results from the deflection measurements of the 249.5 MHz beam.

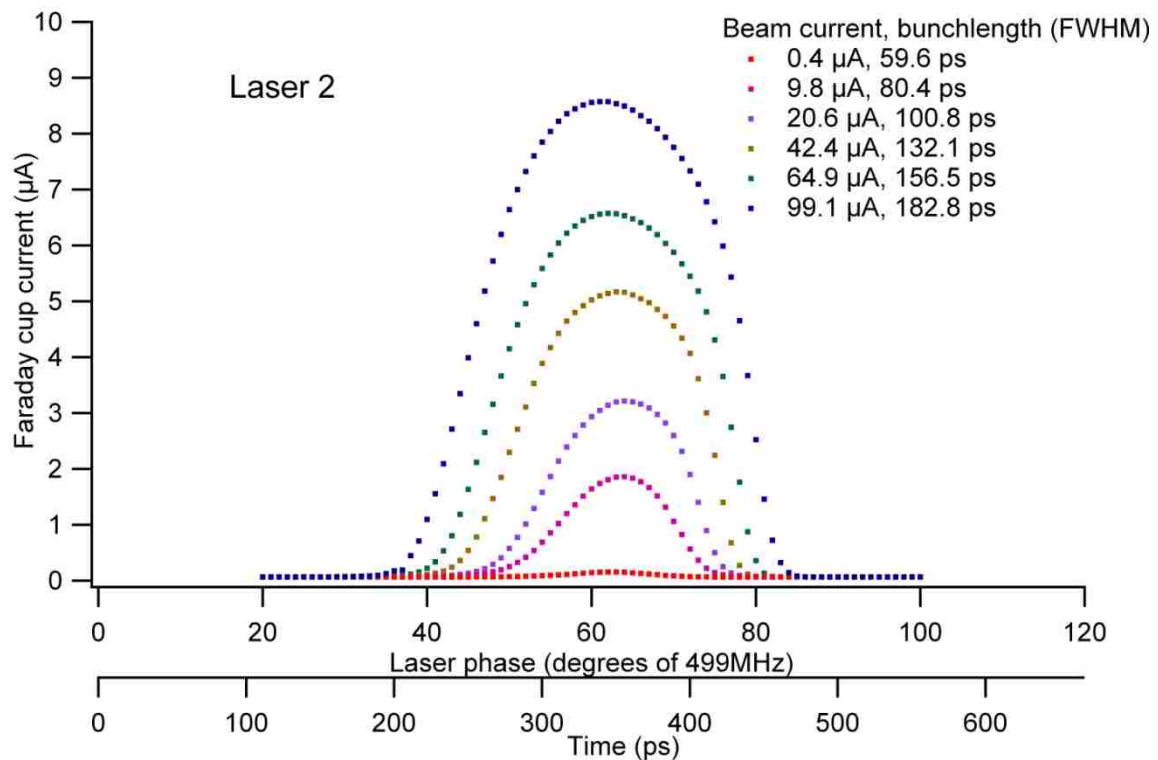


Figure 3.7.1: Deflection measurements of the 249.5 MHz beam.

Laser 2 creates a 60 ps FWHM Gaussian pulse shape. The charge per bunch of the 249.5 MHz beam is double that of the 499 MHz beam contributing to the evolution of its bunch shape as it travels from the cathode to the chopping slit.

3.8: Measurements of the 249.5 MHz with a harmonic cavity

Figure 3.8.1 presents the results from the harmonic cavity measurements of the 249.5 MHz beam.

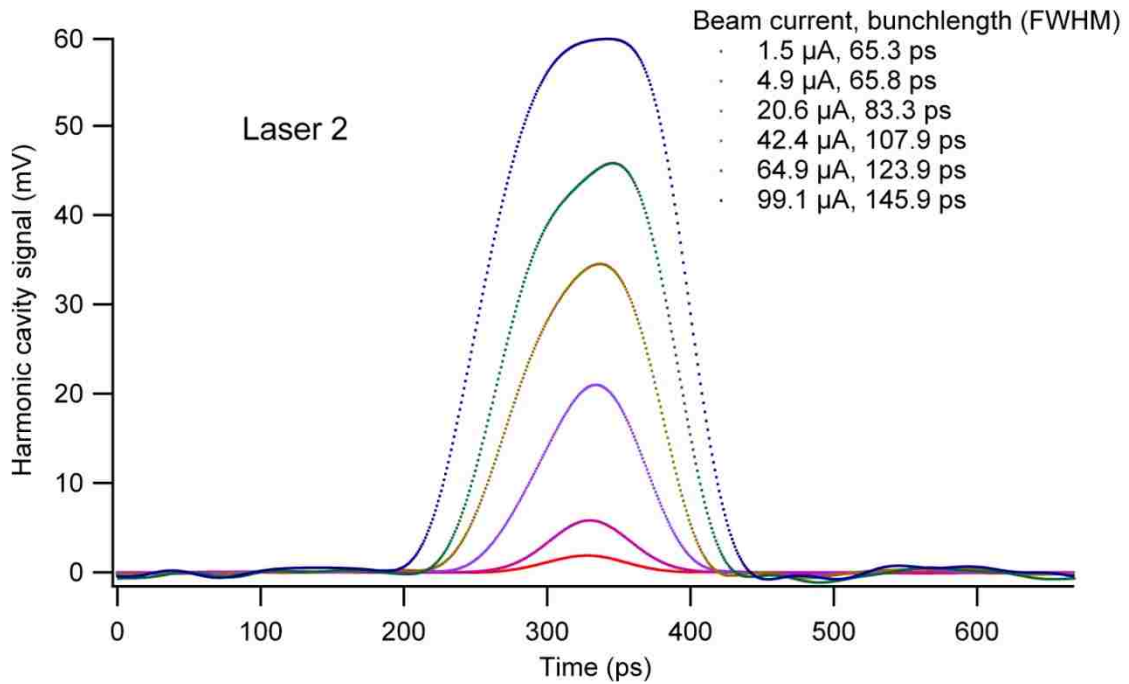


Figure 3.8.1: Harmonic cavity measurements of the 249.5 MHz beam.

The harmonic cavity produces temporal data that is comparable to the RF cavity deflection technique and is non-invasive and is in real time.

3.9 Measurement of an interleaved 499 MHz beams using a 1497 MHz harmonic cavity

Two 10 μ A, 130 kV, 499 MHz beams were created by directing two independently controllable pulsed lasers onto the photocathode in CEBAF's DC photogun. This beam travelled 4 meters down the injector beamline where it passed through the bore of a 1497 MHz harmonic cavity.

Oscilloscope traces were captured for the A and B beam alone, and with both the A and B together as the B beam stepped in 10° increments. The most successful transfer function was created using the DFT of the B beam alone and a 75 ps Gaussian. Figures 3.9.1-3.9.10 present oscilloscope traces of two interleaved beams with various phase differences and their corresponding waveforms of bunch coincidence.

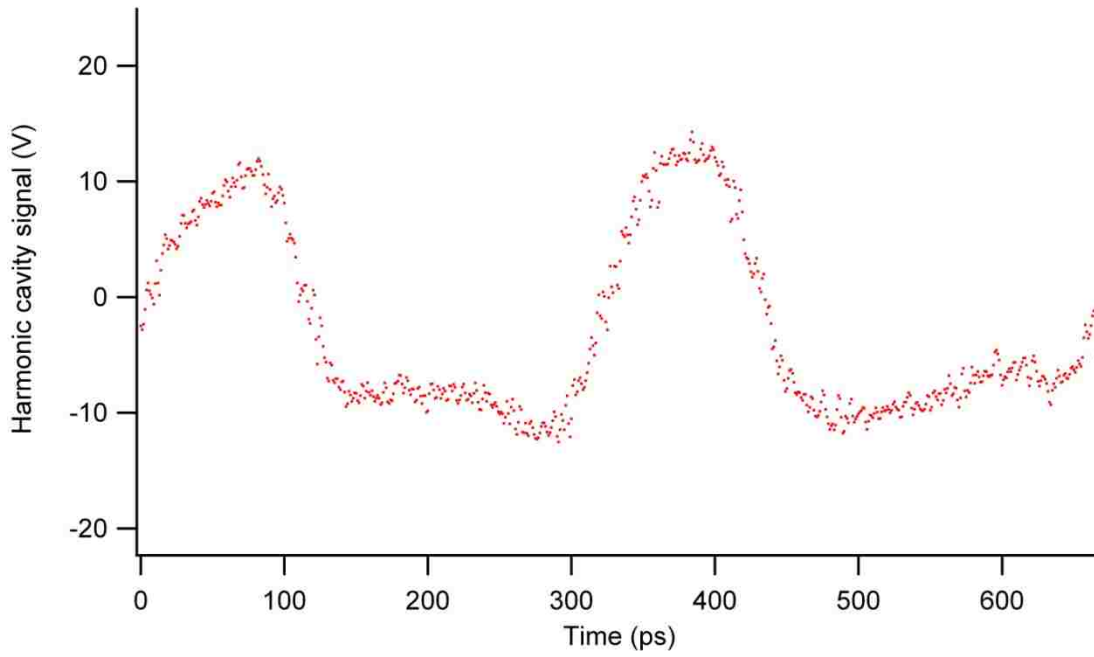


Figure 3.9.1: Two interleaved 499 MHz beams about 40° out of phase.

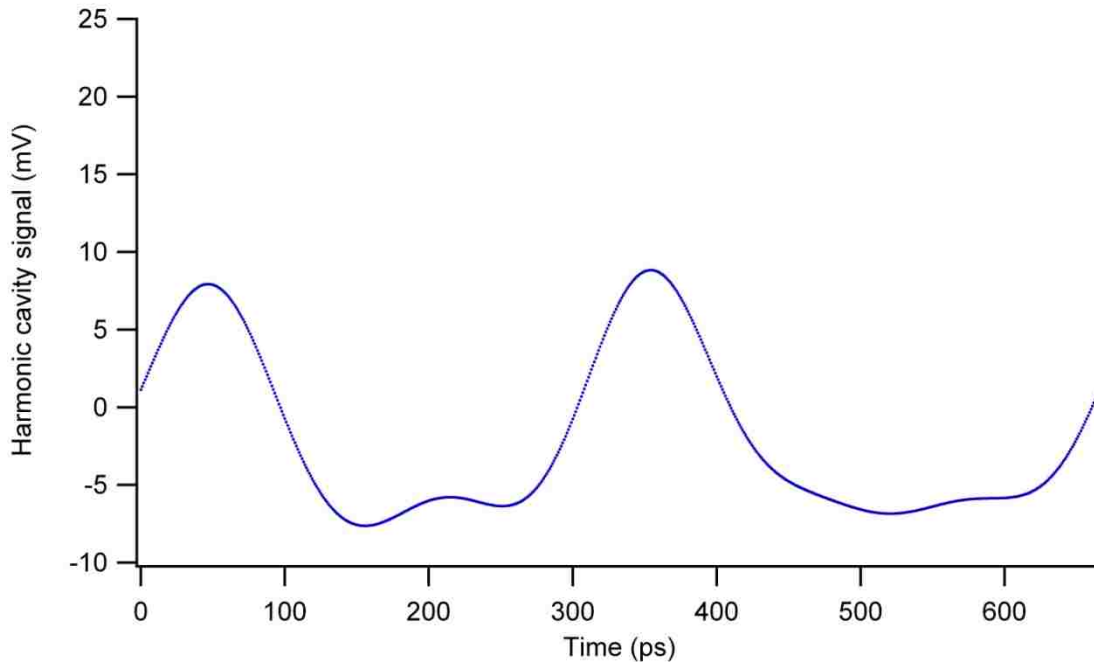


Figure 3.9.2: Processed waveform is nearly 120° from bunch coincidence.

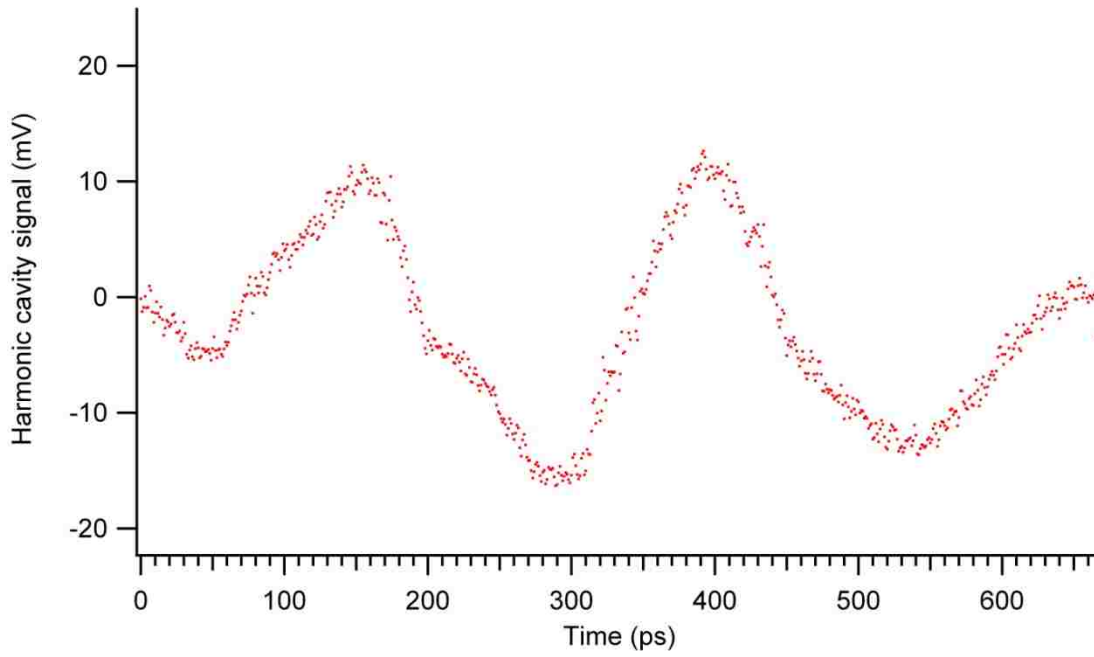


Figure 3.9.3: Two interleaved 499 MHz beams about 30° out of phase.

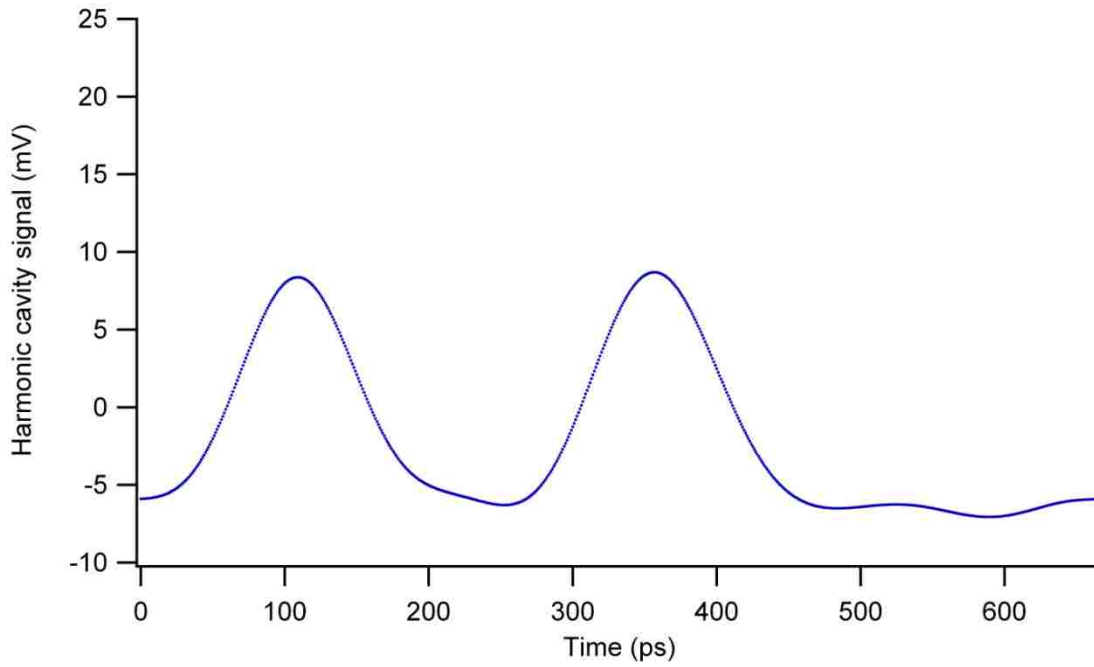


Figure 3.9.4: Processed waveform is near 90° from bunch coincidence.

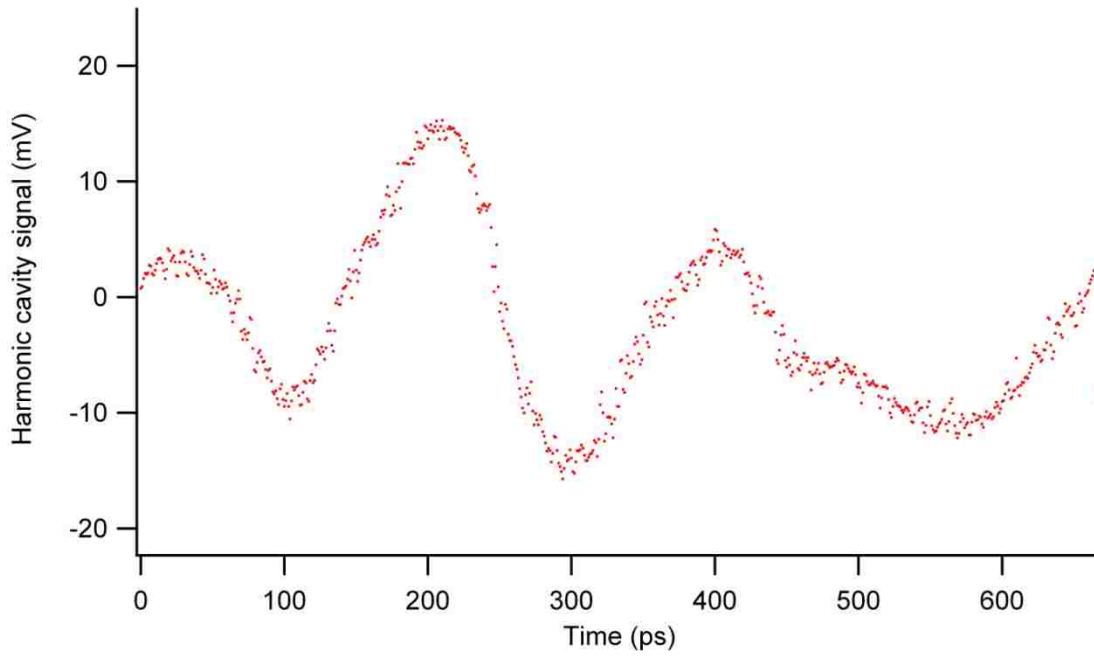


Figure 3.9.5: Two interleaved 499 MHz beams about 20° out of phase.

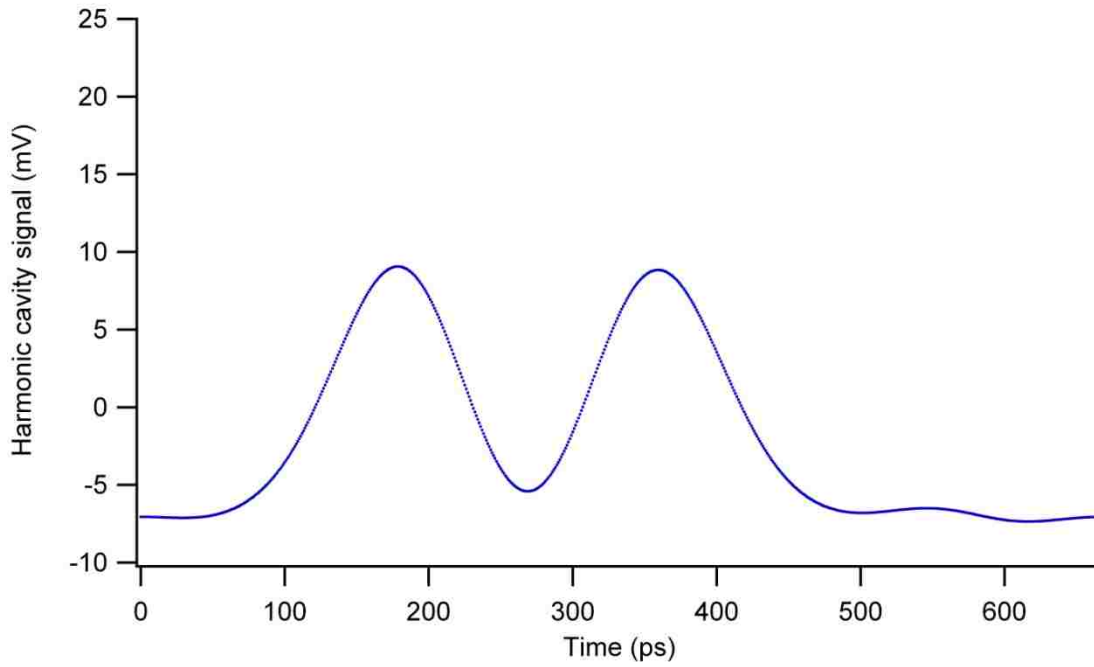


Figure 3.9.6: Processed waveform is near 60° from bunch coincidence.

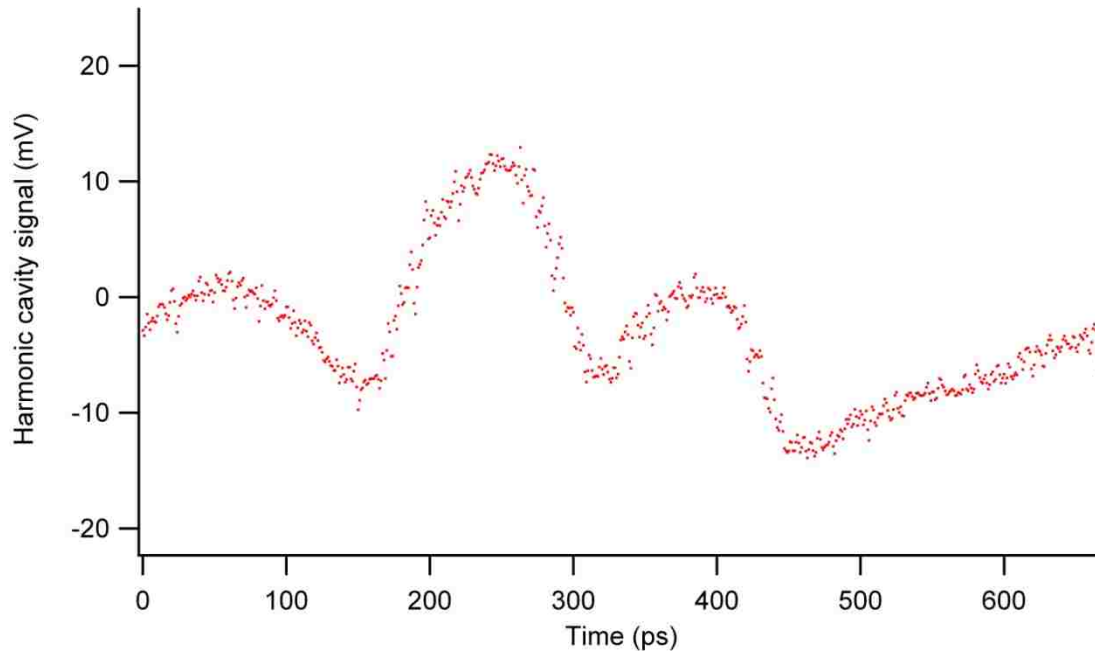


Figure 3.9.7: Two interleaved 499 MHz beams about 10° out of phase.

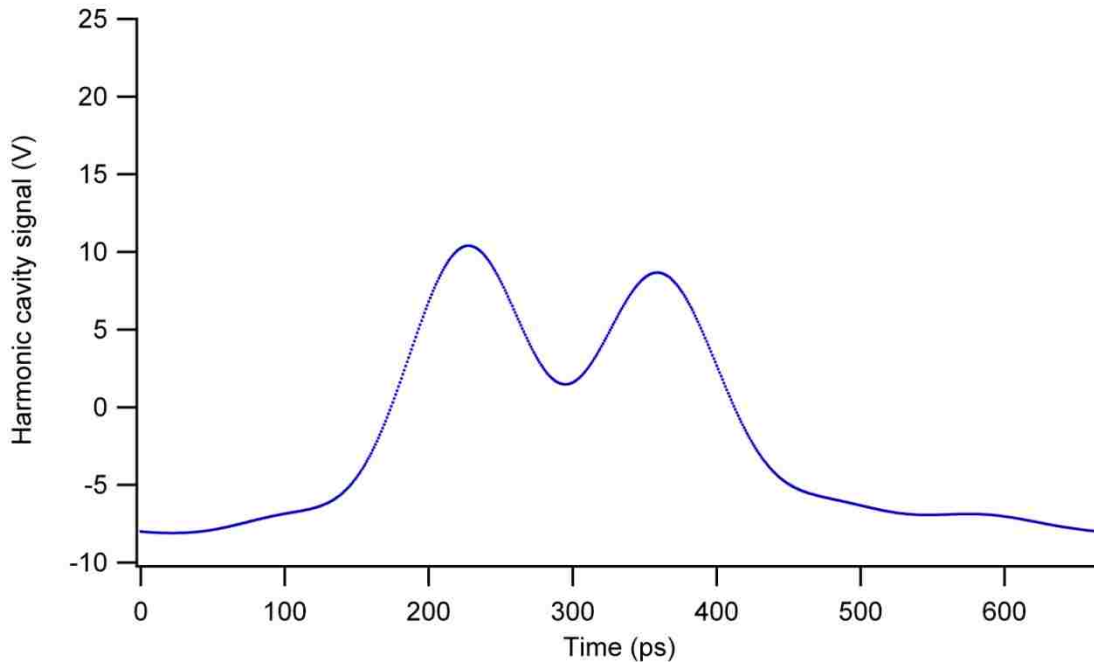


Figure 3.9.8: Processed waveform near 30° from bunch coincidence.

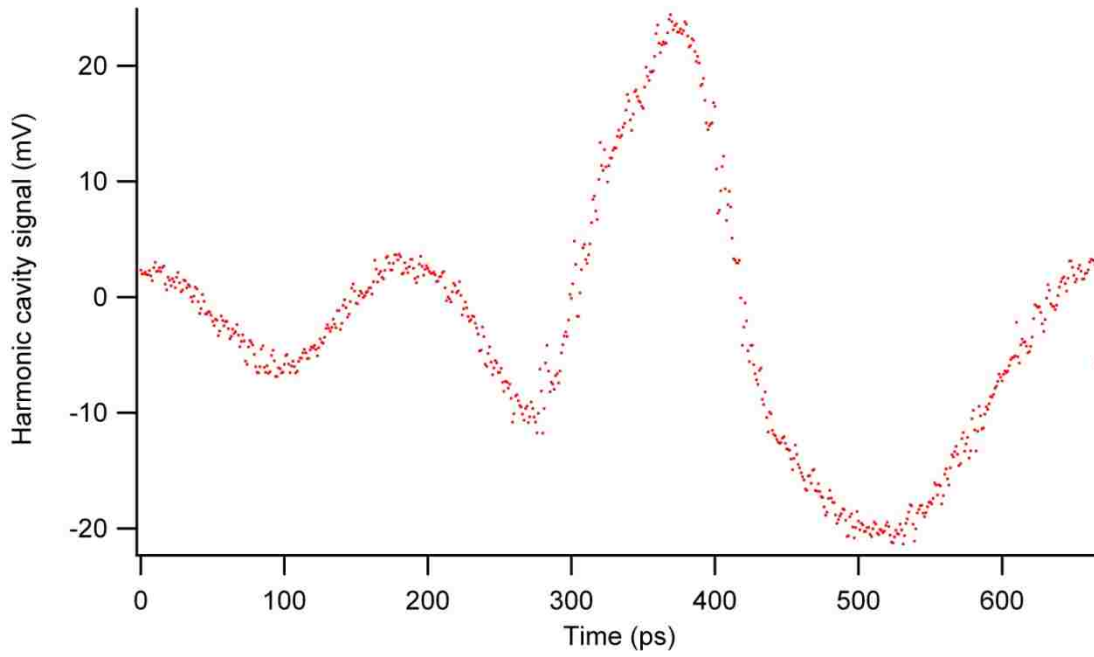


Figure 3.9.9: Two interleaved 499 MHz beams in phase.

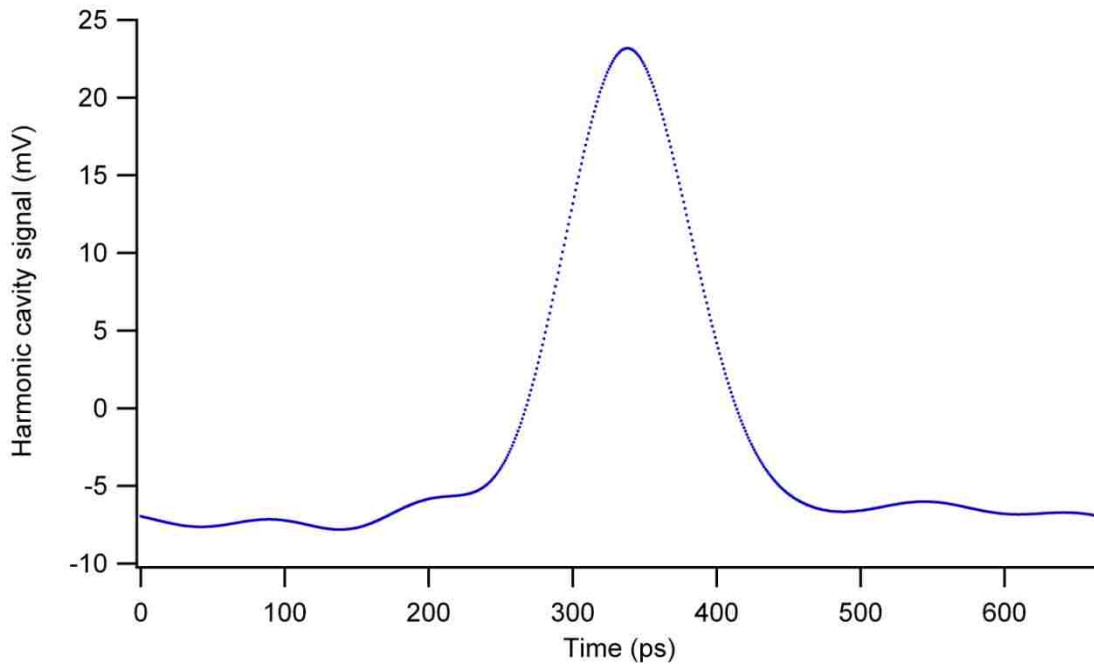


Figure 3.9.10: Processed waveform at bunch coincidence.

While the 1497 MHz harmonic cavity is able to measure beams that are interleaved 499 MHz beams, 10° phase shifts of the 499 MHz beams resulted in 30° phase shifts in the detected 1497 MHz waveforms. This and other ramifications of measuring subharmonic bunch rates are reviewed in Chapter 4.

3.10 Measuring interleaved bunch alignment with an RF detector

An RF detector, also known as a Shottkey diode or as a crystal detector, was attached to the harmonic cavity's output and monitored with a voltmeter as two 499 MHz beams passed through the harmonic cavity. The detected waveform in Figure 3.10.1 repeats as one 499 MHz beam is stepped 120° relative to the other.

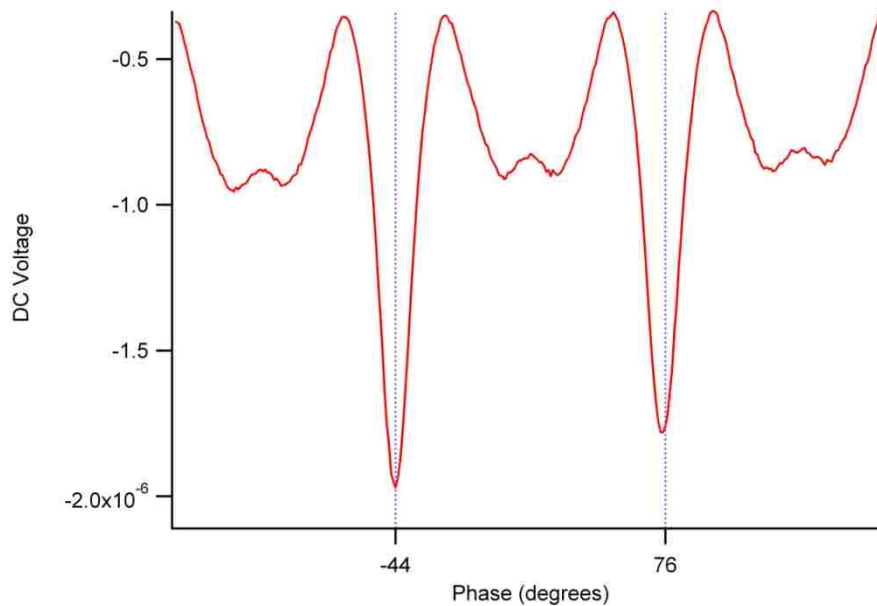


Figure 3.10.1: DC voltage vs. relative phase of two 499 MHz beams.

The waveform of Figure 3.10.1 can be also be created using the detected waveforms of Figures 3.9.1, 3.9.3, 3.9.5, 3.9.7, and 3.9.9, and calculating each

waveforms' DFT and summing the magnitude of each resonance in each measurement and plotting vs. phase. The negative going RF detector spikes in the waveform appear sharply at 120° increments and indicate 120° spacing with the stationary bunch. This and other ramifications of measuring subharmonic bunch rates are reviewed in Chapter 4.

The crystal detector rectifies RF that is coupled out of the resonant modes of the harmonic cavity, producing a negative DC voltage that is proportional to the sum of the magnitude of each of the cavity's resonances. To simulate the measured DC an ideal harmonic cavity would produce when these beams pass through it, the magnitude of each two bunch waveform's FT was calculated. The measurement made by the crystal detector is modeled by summing the magnitude of each harmonic term and multiplying by -1 (negative going detector).

Key Concept #7: A harmonic cavity and a Schottky diode can be used to measure the relative phasing of interleaved beams.

3.11 500 kV Measurements

Downbeam of the chopping system, the CEBAF injector has an RF buncher cavity and what is called "the capture section" that accelerates the beam from 130 kV to 500 kV and sends the beam into the superconducting accelerator.

The buncher and capture sections of the CEBAF injector were energized to produce the shortest electron bunches possible. A 500 kV beam passed through the harmonic cavity with bunches estimated to be 1-10 ps FWHM in duration. The magnitude of the DFT of the detected waveform can be used to observe the harmonic

frequency content in the detected signal and the bandwidth of the cavity. The cavity has at least 13 harmonic modes and operates up to 20 GHz. Figure 3.11.1 shows the detected waveform from a 500 kV, 499 MHz beam and Figure 3.11.2 shows the relative magnitude of the harmonic cavity's resonances.

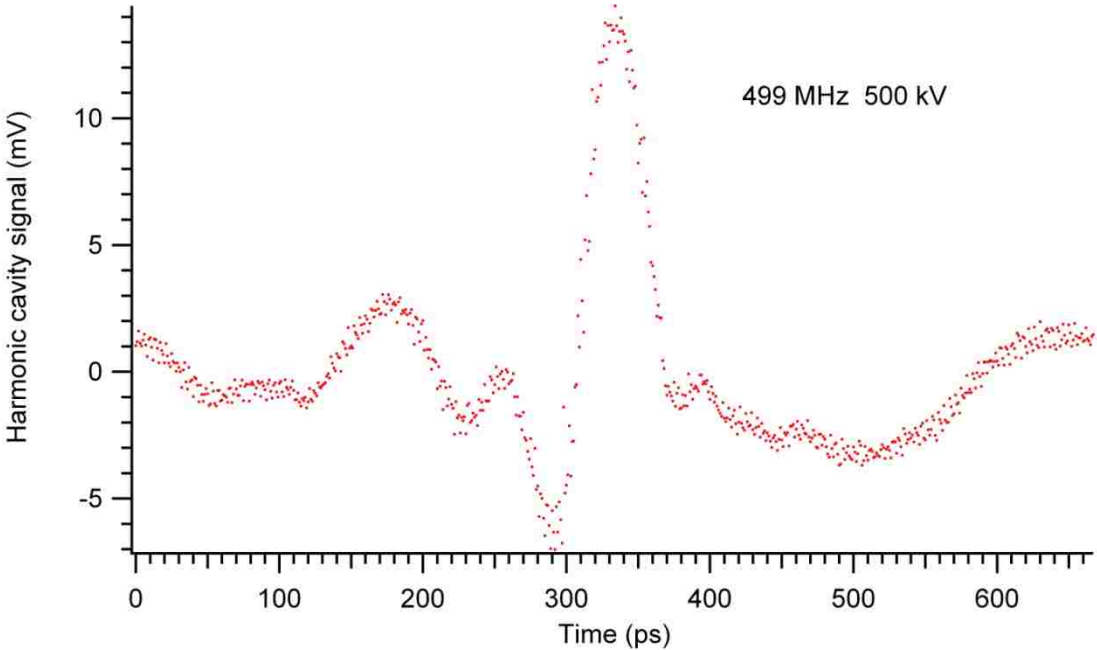


Figure 3.11.1: The detected waveform from a 500 kV, 499 MHz beam.

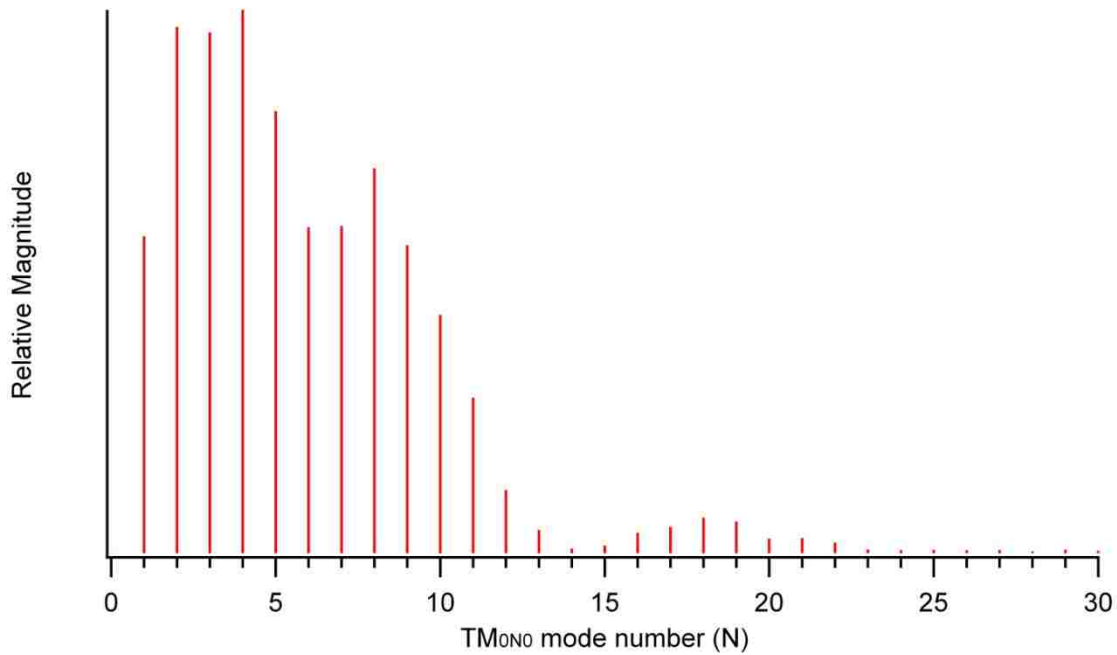


Figure 3.11.2: The relative magnitude of the harmonic cavity’s resonances.

The harmonic cavities bandwidth, or number of operating TM_{0NO} modes, determines the brevity of beam features that it can detect. The harmonic cavity described in Chapter 2 had ten operating harmonic modes, demonstrating that improvements in cavity design and fabrication techniques increase bandwidth. It is anticipated that this trend will continue and future harmonic cavities will provide more accurate measurements of briefer bunches.

CHAPTER 4 KEY CONCEPTS AND CONCLUSION

4.1 Subharmonic measurements

A 499 MHz beam is described in a Fourier series as a series of harmonics of 499 MHz. A 1497 MHz harmonic cavity can only respond to every third term of the beam's excitation. This phenomenon can be investigated graphically by creating an arbitrary bunch shape with a period of the beam of interest, calculating its DFT, and then calculating its inverse transform using only the terms that are harmonics of the cavity's fundamental frequency. Figure 4.1.1 is a hypothetical 499 MHz beam that is divided into three periods of 1497 MHz (a,b, and c). Figure 4.1.2 is the same waveform after calculating its DFT, and then calculating its inverse transform using only harmonic terms that are integer multiples of 1497 MHz. The result is equivalent to the superposition of (a) and (b) and (c).

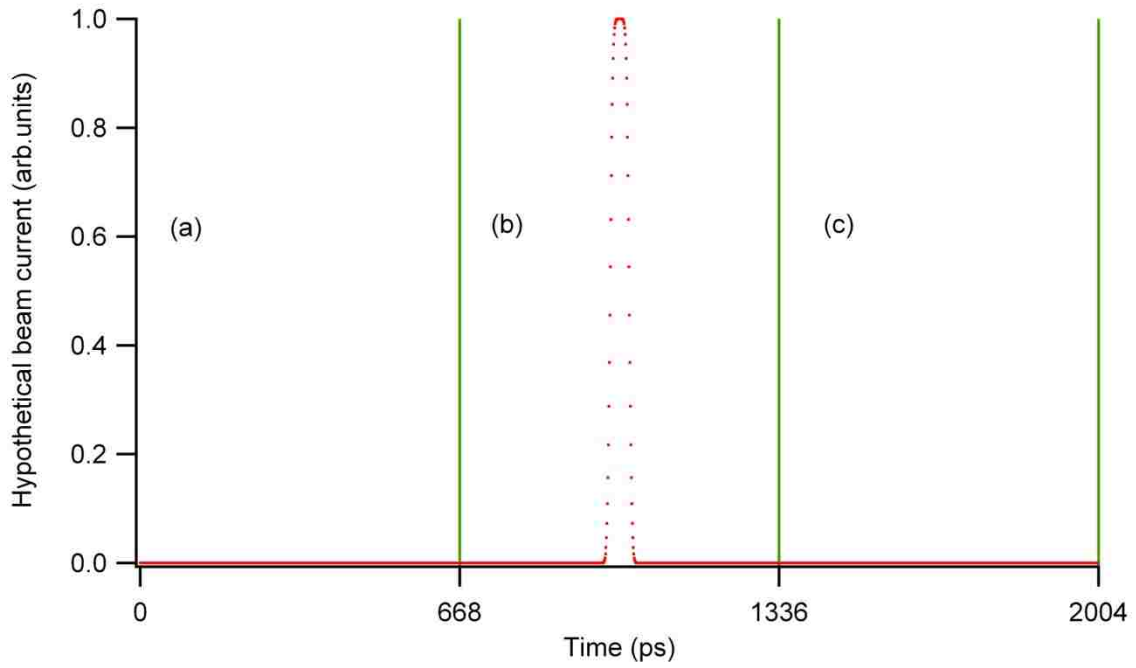


Figure 4.1.1: A hypothetical 499 MHz beam with a 2004 ps period.

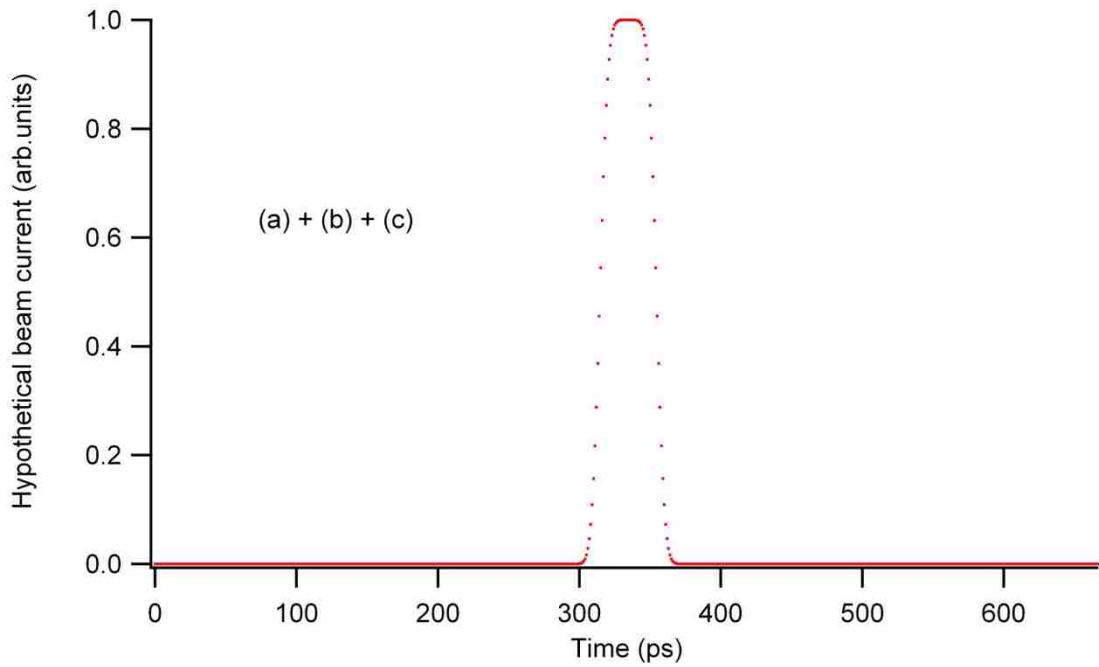


Figure 4.1.2: The IFT of every third term of waveform of Figure 4.1.1's DFT.

The result of a subharmonic measurement is in an undistorted bunch shape in Figure 4.1.2 having the period of the 1497 MHz cavity. Because the effect is equivalent to superimposing the three sections of the 499 MHz beam (a), (b), and (c), the exact bunch location is indeterminate.

Key Concept #8: Subharmonic measurements can be simulated by creating an arbitrary bunch shape with a period of the beam of interest, calculating its DFT, and then calculating its inverse transform using only the terms that are harmonics of the cavity's fundamental frequency.

4.2 Key concepts

1) The waveform exported from the cavity's antenna and detected by the oscilloscope is the superposition of the cavity's resonant modes excited by the beam and coupled out of the cavity.

2) The relative amplitude and phase of each individual harmonic cavity mode as it is coupled out of the cavity can be determined from the detected waveform, by calculating the waveform's DFT of one wavelength of the signal.

3) Distortion in the detected waveform is caused by an imperfect antenna, an imperfect harmonic cavity, and cable dispersion.

4) The harmonic cavity's transfer function can be used to correct distortion.

5) The harmonic cavity's transfer function is the ratio of two Fourier series, one is the Discrete Fourier series of a brief detected waveform, and the other is the Discrete Fourier series of the true beam current.

6) The harmonic cavity's transfer function can be estimated, tested, and refined by the method of blind deconvolution.

7) A harmonic cavity and a Schottkey diode can be used to measure the relative phasing of interleaved beams.

8) Subharmonic measurements can be simulated by creating an arbitrary bunch shape with a period of the beam of interest, calculating its DFT, and then calculating its inverse transform using only the terms that are harmonics of the cavity's fundamental frequency.

4.3 Conclusion

A cavity designed to have multiple harmonic TM_{0N0} modes can be used to accurately measure the longitudinal profile of a bunched charged particle beam passing through its bore, non-invasively, and in real time.

Multi-harmonic TM_{0N0} cavities were designed, constructed, and beamline tested in a variety of experiments at the Thomas Jefferson National Accelerator Facility (TJNAF or Jlab). Measurements with a sampling oscilloscope provided signals that resemble the profile of electron bunches passing through the cavity's bore.

Straightforward signal processing techniques reduce distortion in the measurement and provide real time profiles of electron bunches with picosecond accuracy. Subharmonic

beams having bunch repetition rates of $1/3^{\text{rd}}$ and $1/6^{\text{th}}$ of Jlab's 1497 MHz bunch frequency, and interleaved sub-harmonic beams were also measured. Comparison between measurements made using a harmonic cavity were corroborated with an established invasive measurement method and with computer models.

Future work will include improving design and fabrication techniques of harmonic cavities to increase their bandwidths. Further development of computer controlled harmonic drivers will create new applications for harmonic cavities when actively driven by RF, such as bunching or bunch shaping. Development of an automated blind deconvolution algorithm will improve the estimates of the harmonic cavities transfer function so that processed waveforms will more accurately represent true bunch profiles.

APPENDIX A - Faraday Cup award.



Ctra. BP-1413, Km. 3.3
08290 Cerdanyola del Vallès
Barcelona - Spain

Tel. (+34) 93 592 4300
Fax (+34) 93 592 4301
www.albasynchrotron.es

Brock Roberts
Electrodynamic
4909 Paseo Del Norte Ne Suite D,
Albuquerque, New Mexico 87113, USA
brockr@unm.edu

April 4th, 2016

Dear Brock Roberts,

As Committee Chairs of the 2016 International Beam Instrumentation Conference (IBIC 2016, www.ibic2016.org), we are very pleased to inform you that your work on "Compact noninvasive electron bunch-length monitor" has been chosen by the IBIC 2016 Scientific Committee as the 2016 Faraday Cup award winner.

Since the merging of the American BIW and the European DIPAC conferences into the, now, International Beam Instrumentation Conference, IBIC, this price is sponsored by the conference itself. This is the first time the Faraday Cup is awarded in this new model.

The award will be presented to you on Monday, September 12th at 14:30 during the IBIC 2016 held in the World Trade Center in Barcelona, Spain. Following, we expect you to present your work as an invited talk of 20 minutes.

The award includes a Commemorative Diploma, a 1000€ price and the free registration to the conference.

On behalf of the entire program committee, I sincerely hope that you can join us for IBIC 2016 in Barcelona, present your work to the conference attendees, and accept your well-deserved award.

Yours sincerely,

Francis Perez, Conference Chair
Ubaldo Iriso, Scientific Chair

International Beam
Instrumentation
Conference **IBIC**
11 - 15 September 2016 Barcelona



1 de 1

International Beam Instrumentation Conference **IBIC**

11 - 15 September 2016 Barcelona



The Scientific Committee of the
2016 International Beam Instrumentation Conference awards

Mr. Brock Franklin Roberts

for his work on

"Compact non-invasive electron bunch-length monitor"

as the

2016 Faraday Cup Winner

Francis Perez, IBIC 2016 Conference Chair

A handwritten signature in black ink, appearing to be "FP", written over a horizontal line.

Ubaldo Iriso, IBIC 2016 Scientific Chair

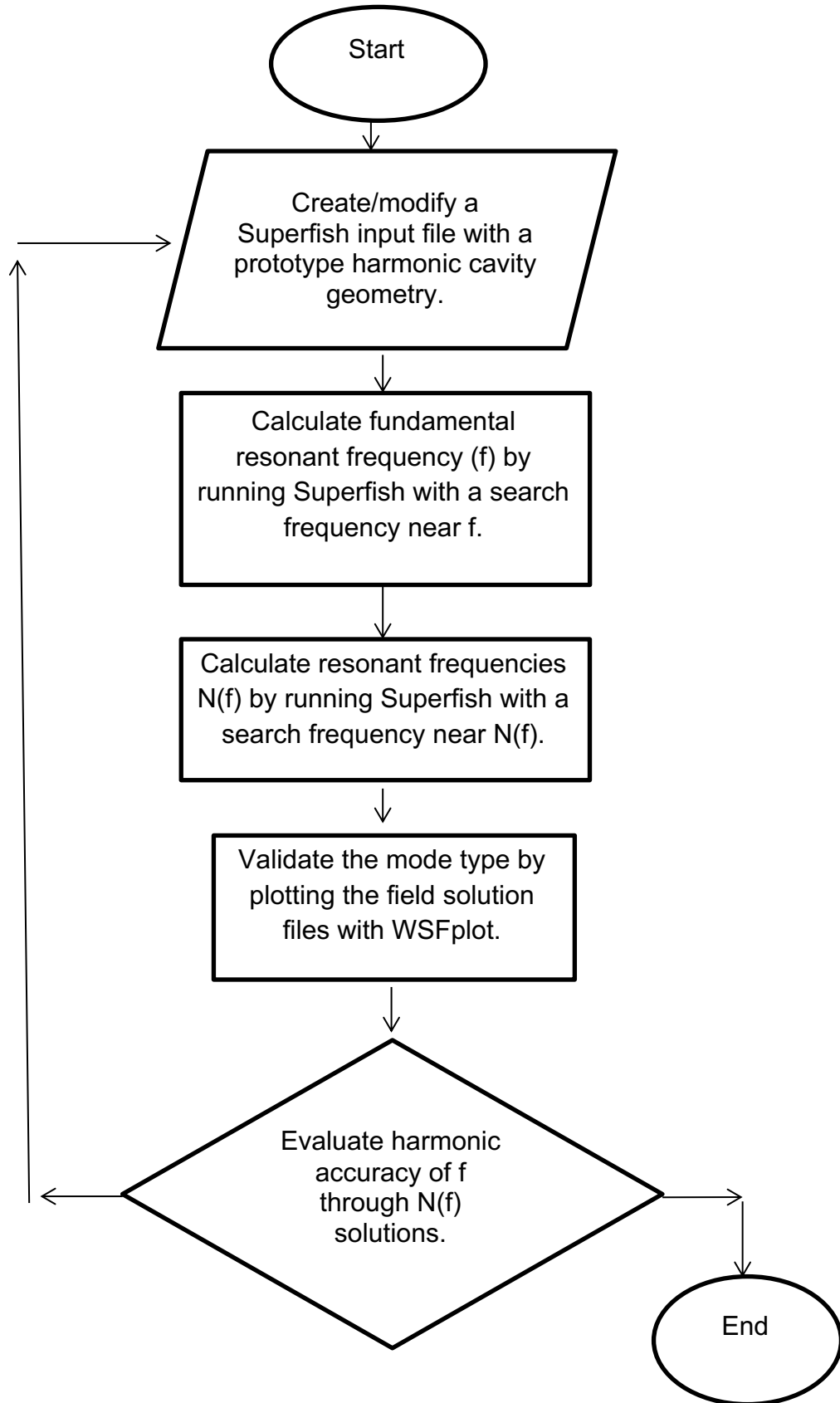
A handwritten signature in black ink, appearing to be "UI", written over a horizontal line.

APPENDIX B – Publications

[1] B. Roberts, R.R. Mammei, M. Poelker, and J.L. McCarter, “Compact Noninvasive Electron Bunch-Length Monitor,” *Phys. Rev. ST Accel. Beams* **15**, 122802 (2012).

[2] B. Roberts, F. Hannon, M.M. Ali, E. Forman, J. Garmes, R. Kazimi, W. Moore, M. Pablo, M. Poelker, A. Sanchez, and D. Speirs, “Harmonically Resonant Cavity as a Bunch Length Monitor,” *Phys. Rev. Accel. Beams* **19**,052801 (2016).

APPENDIX C- Design Flowchart



APPENDIX D – US patent 9,385,412 for “Harmonic cavity resonator”



US009385412B2

(12) **United States Patent**
Roberts

(10) **Patent No.:** **US 9,385,412 B2**
(45) **Date of Patent:** **Jul. 5, 2016**

(54) **HARMONIC CAVITY RESONATOR**

7,463,121 B2 * 12/2008 D’Ostilio H01P 7/04
333/207

(71) Applicant: **Brock F Roberts**, Albuquerque, NM
(US)

* cited by examiner

(72) Inventor: **Brock F Roberts**, Albuquerque, NM
(US)

Primary Examiner — Robert Pascal
Assistant Examiner — Kimberly Glenn

(*) Notice: Subject to any disclaimer, the term of this patent is extended or adjusted under 35 U.S.C. 154(b) by 0 days.

(57) **ABSTRACT**

Cavity resonators have a multitude of applications in radio-frequency, microwave, and vacuum electronics. Cavity resonators are used as frequency selective filters and oscillators. In vacuum electronic devices and charged particle accelerators cavities are used to couple energy into and out of charged particle beams. Typically cavity resonators are optimized for single mode operation and are limited to sinusoidal waveforms and interactions. Harmonic cavities have many of the same applications, but because they resonate many axially symmetric harmonic modes simultaneously, the superposition of these modes is an on-axis arbitrary waveform. Harmonic cavities have both passive and active applications. When a periodic charged particle beam passes through a harmonic cavity whose resonances are at the same frequency as the beam’s periodicity, the beam induces these cavity modes to resonate. The superposition of these modes, on axis, has a voltage vs. time waveform that ideally mirrors the current vs. time of the beam that induced it. Harmonic cavities can also be used to apply arbitrary waveforms to charged particle beams when driven externally. These waveforms can be used to modulate, shape, and accelerate the beam. A harmonic cavity whose axis is tilted to the beamline can be used to change the trajectory of selected particle bunches by delivering them fast kicking pulses.

(21) Appl. No.: **13/998,924**

(22) Filed: **Dec. 23, 2013**

(65) **Prior Publication Data**
US 2016/0141743 A1 May 19, 2016

(51) **Int. Cl.**
H01P 7/06 (2006.01)

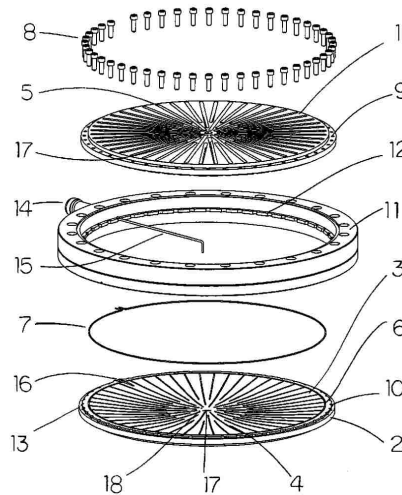
(52) **U.S. Cl.**
CPC **H01P 7/06** (2013.01)

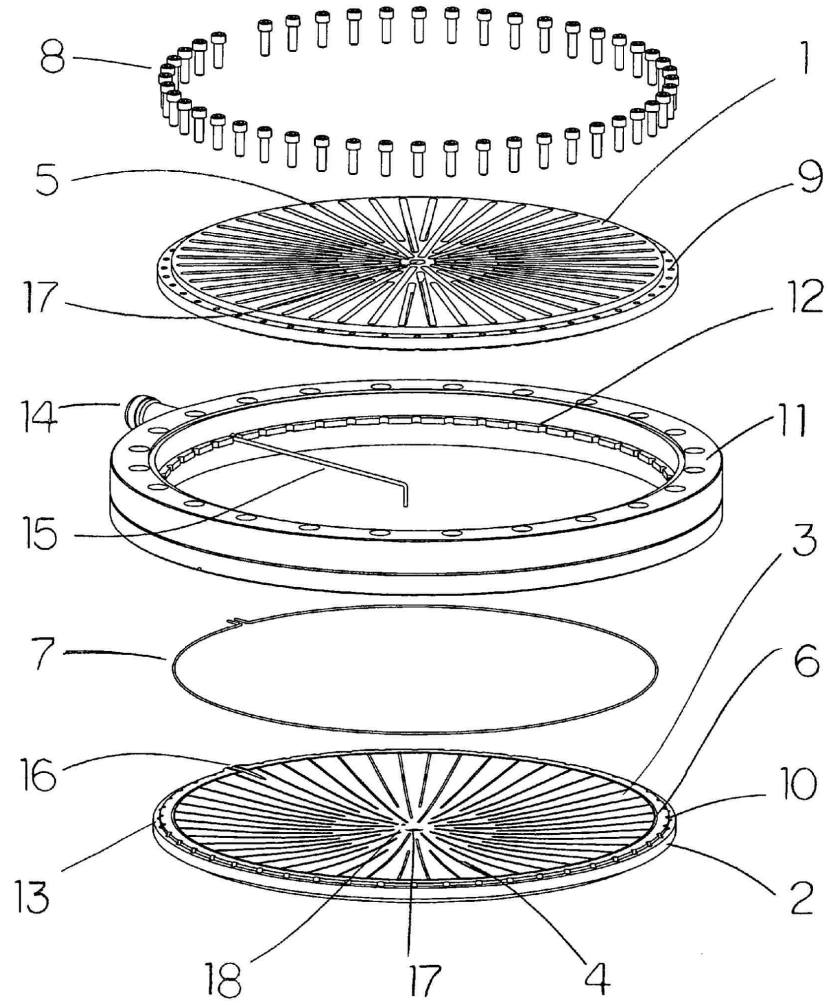
(58) **Field of Classification Search**
CPC H01P 7/06; H01P 1/208; H01P 1/2082
USPC 333/227–233
See application file for complete search history.

(56) **References Cited**
U.S. PATENT DOCUMENTS

2,907,913 A * 10/1959 Dench H01J 25/40
313/158
3,471,738 A * 10/1969 Bert H01J 23/24
315/3.5

2 Claims, 1 Drawing Sheet





HARMONIC CAVITY RESONATOR

BACKGROUND

Cavity resonators are efficient, robust, electromagnetic devices that have a multitude of applications in radio-frequency, microwave, and vacuum electronics. Cavity resonators are used as frequency selective filters and oscillators. In vacuum electronic devices and charged particle accelerators cavities are used to couple energy into and out of charged particle beams. In the vast majority of these applications, only the fundamental frequency of the cavity resonator is utilized. The fundamental cavity mode generally has the greatest frequency separation from neighboring modes, has a simple field distribution, and can easily be made to be axially symmetric for interacting with an on-axis beam. The higher order modes in most cavity geometries are a mixture of transverse electric (TE) and transverse magnetic (TM) modes that increase in density with frequency until becoming a continuum. The mode spacing and fields of higher order modes are irregular and are generally undesirable in most applications. Applications that use single mode cavities are limited to sinusoidal waveforms and interactions.

Advantages

Harmonic cavities are designed to have many periodic axially symmetric transverse magnetic modes that can resonate simultaneously. Fourier's theorem summarizes the idea that any periodic function can be created by the superposition of harmonic sinusoidal waves. Because harmonic cavities can resonate multiple harmonic sinusoidal modes simultaneously, and because these modes are axially symmetric, a harmonic cavity can resonate an axial arbitrary waveform, limited in fidelity by its number of harmonic modes.

Harmonic cavities can be used as non-invasive beam monitors. When a periodic charged particle beam passes through a harmonic cavity whose resonances are at the same frequency as the beam's periodicity, the beam induces these cavity modes to resonate. The relative amplitude and phases of these modes are a manifestation of the beam's Fourier series. The superposition of these modes, on axis, has a voltage vs. time waveform that ideally mirrors the current vs. time of the beam that induced it.

Harmonic cavities have applications when driven externally with microwave energy. When several harmonics are driven simultaneously, the cavity's axial voltage vs. time is the superposition of these harmonics. Control of the amplitude and phase of these harmonics controls the cavity's axial voltage vs. time. These waveforms can be used to interact with a charged particle beam passing through the harmonic cavity's axial bore. Beam modulation, bunch shaping, and accelerating waveforms can be created and tailored by superimposing multiple harmonic modes within a harmonic cavity. A harmonic cavity whose axis is tilted to the beamline can be used to change the trajectory of selected particle bunches by delivering them fast kicking pulses.

DRAWINGS FIGURE

FIG. 1 is an exploded view of an embodiment of the invention.

REFERENCE NUMERALS IN DRAWING

- 1. cavity half A
- 2. cavity half B

- 3. saucer shape
- 4. radial slits
- 5. widened slits
- 6. wire groove
- 7. wire seal
- 8. fasteners
- 9. through-holes
- 10. threaded holes
- 11. vacuum flange
- 12. retaining ridge
- 13. relief for retaining ridge,
- 14. coaxial feedthrough
- 15. wire antenna
- 16. coaxial bore
- 17. beam bore
- 18. antenna termination

DESCRIPTION OF THE INVENTION

The harmonic cavities conductive enclosure is created by machining and assembling two metal cavity halves, (1) and (2), such that when assembled, the resultant cavity is a predetermined saucer shape (3). Thin radial slits (4) are cut through the cavity walls, and are widened (5) from behind the cavities interior surface. A semicircular cross section wire groove (6) is machined outside of the cavities perimeter in both halves to capture a wire seal (7). The harmonic cavity is assembled by passing fasteners (8), through through-holes (9) around the periphery of cavity half A (1), into threaded holes (10) in cavity half B (2). The wire seal (7) is compressed by tightening these fasteners (8).

A vacuum flange (11) with a retaining ridge (12) houses the harmonic cavity. A relief for the retaining ridge (13) is cut out of each cavity half, (1) and (2), so that the assembled cavity is retained within the vacuum flange. A vacuum coaxial feedthrough (14) penetrates the edge of the vacuum flange whose center conductor transitions into a wire antenna (15). The wire antenna enters the cavity through a coaxial bore (16) drilled through the cavities plane of symmetry toward the beam bore (17) where it bends parallel to the cavity axis and connects to ground at the antenna termination (18).

OPERATION OF THE INVENTION

The harmonic cavity resonator is designed to exclusively resonate many axially symmetric harmonic transverse magnetic (TM) modes. The cavities first, or fundamental mode is the TM_{010} mode. Harmonic cavity resonators are designed such that the frequencies of the higher order axially symmetric transverse magnetic modes (TM_{020} , TM_{030} , etc.,) are harmonics of the fundamental. The cavity can be scaled in size to change its fundamental frequency.

The design of harmonic cavities relies on three criteria. Firstly, the cavity design excludes TE modes. A thin saucer-shaped cavity has a mode spectrum clear of TE modes for a wide bandwidth because TE modes resonate at frequencies $\geq c/2h$ where h is the cavities axial length. Secondly, the shape (3) of the cavity was designed so that the TM_{0ND} modes are harmonic. This was accomplished by iteratively modifying the cavity's geometry and solving for the TM_{0ND} mode frequencies with a 2-D electromagnetic field solver. Finally radial slits (4) cut into the cavities interior surface prevent the resonance of non-axially symmetric TM modes. The TM_{0ND} modes have purely radial wall currents and are unaffected by these slits while the TM_{MNP} modes with azimuthal mode numbers (M) less than the number of discontinuities are removed from the cavity's mode spectrum.

3

The preferred embodiment of the invention is assembled within a vacuum flange (11) to facilitate its inclusion into experimental apparatus. The radial slits (4) are widened behind the cavities surface (5) to increase vacuum conductance. The wire seal (7) provides an electrically conductive union between the two cavity halves and can be used as a tuning mechanism. Plastic deformation of the wire seal (7) slightly changes the cavities harmonic frequency by slightly decreasing its outer radius. The harmonic cavity shape (3) is relatively insensitive to scaling in axial length, providing design options for different applications. Thicker saucer shaped harmonic cavities have resonances with higher quality factors, but are limited in bandwidth by TE modes entering their mode spectrum. The thinner saucer shaped cavities have less efficient resonances, but have the widest bandwidth.

The vacuum coaxial feedthrough (14) has a bandwidth sufficient to exchange energy with the cavities harmonics and transitions into a wire antenna (15). The wire antenna enters the cavity through coaxial bore (16) drilled through the cavities plane of symmetry toward the beam bore (17) where it bends parallel to the cavity axis and connects to ground and is retained (18). Manipulating the height and curvature of this loop can be used to adjust mode coupling. A bore (17) through the cavities axis of symmetry allows for energy exchange between the cavities modes and charged particle beams. Because TM_{0n0} cavity modes are axially symmetric and have a field maximum on the cavity axis, they all interact with a passing beam.

Harmonic cavities can be used as a non-invasive beam monitors. When a periodic charge particle beam passes through a harmonic cavity whose resonances are at the same frequency as the beam's periodicity, the beam induces these cavity modes to resonate. The relative amplitude and phases of these modes are a manifestation of the beam's Fourier series. The superposition of these modes, on axis, has a voltage vs. time waveform that ideally mirrors the current vs. time of the beam that induced it. This waveform is coupled from the modes induced by the beam to the antenna (15), and can be measured with a sampling oscilloscope connected to the coaxial feedthrough (14).

Harmonic cavities also have applications when their modes are driven by externally generated microwave energy. When many harmonics are driven simultaneously, the cavity's axial voltage vs. time is the superposition of these harmonics. Control of the amplitude and phase of these harmonics controls the cavity's axial voltage vs. time. This arbitrary waveform can be used to interact with charged particle beams

4

passing through the harmonic cavities axial bore (17). Beam modulation, acceleration, and bunch shaping waveforms can be created and tailored by superimposing multiple harmonic modes within a harmonic cavity. A harmonic cavity whose axis is tilted to the beam line can be used to change the trajectory of selected particle bunches by delivering them fast kicking pulses.

Harmonic cavities can also be used as filters; a harmonic cavity with two antenna's communicating through the cavities resonance's will only pass complex high speed arbitrary waveforms with the same frequency as the cavities fundamental.

CONCLUSIONS RAMIFICATIONS AND SCOPE

Accordingly, the reader will see that there are many advantages to cavity designs that simultaneously resonates many periodic axially symmetric modes. Because these modes are axially symmetric, a harmonic cavity can resonate an axial arbitrary waveform that is either induced by, or designed to interact with, a charged particle beam passing through its bore (17).

While the above description contains many specificities, these should not be construed as limitations on the scope of the invention, but as an exemplification of an embodiment thereof. Many other variations are possible. For example the wire seal (7) could be a brazing alloy, or the assembly could be welded, or the conductive enclosure could be cast as a single piece. The cavity could be filled with a dielectric, the antenna could be a near axis electric field probe, or an electro-optic sensor. The beamline could be tilted relative to the harmonic resonators bore to deliver kicking pulses to selective charge bunches within a beam.

Thus the scope of the invention should be determined by the appended claims and their legal equivalents, rather than by the specifics of the embodiment described.

I claim:

1. A cavity resonator comprising:

- a. A conductive enclosure with a predetermined saucer shape that has many axially symmetric transverse magnetic modes with harmonic resonant frequencies,
- b. means to exchange energy with the cavity resonator,
- c. a plurality of radial slits in said conductive enclosure, whereby exclusively resonating said many axially symmetric harmonic modes.

2. The cavity resonator of claim 1 that has an axial bore.

* * * * *

LIST OF REFERENCES

- [1] B. Roberts, R.R. Mammei, M. Poelker, and J.L. McCarter, "Compact Noninvasive Electron Bunch-Length Monitor," *Phys. Rev. ST Accel. Beams* **15**, 122802 (2012).
- [2] B. Roberts, F. Hannon, M.M. Ali, E. Forman, J. Garmes, R. Kazimi, W. Moore, M. Pablo, M. Poelker, A. Sanchez, and D. Speirs, "Harmonically Resonant Cavity as a Bunch Length Monitor," *Phys. Rev. Accel. Beams* **19**, 052801 (2016).
- [3] S.O. Scriber and D.A. Swenson, "A Single-Cavity Double-Frequency Buncher," *IEEE Trans. Nucl. Sci.* **26**, 3705 (1979).
- [4] K. Halbach and R. F. Holzinger, "SUPERFISH - A Computer Program for Evaluation of RF Cavities with Cylindrical Symmetry," *Part. Accel.* **7**, 213 (1976).
- [5] Y. Huang, H. Wang, R. Rimmer, S. Wang, and J. Guo, "Ultrafast Harmonic RF Kicker Design and Beam Dynamics Analysis for an Energy Recovery Linac Based Electron Circulator Cooler Ring," *Phys. Rev. Accel. Beams* **19**, 084201 (2016).
- [6] Y. Iwashita, "Multi-Harmonic Impulse Cavity," *Proc. 1999 Particle Accelerator Conference* (New York, NY, March 27-April 2, 1999).
- [7] C.A. Balanis, *Advanced Engineering Electromagnetics* (John Wiley and Sons, New York, NY, 2012), p.494.
- [8] Ibid, p.499.
- [9] C. K. Sinclair, P. A. Adderley, B. M. Dunham, J. C. Hansknecht, P. Hartmann, M. Poelker, J. S. Price, P. M. Rutt, W. J. Schneider, and M. Steigerwald, "Development of a High Average Current Polarized Electron Source with Long Cathode Operational Lifetime," *Phys. Rev. ST Accel. Beams* **10**, 023501 (2007).

- [10] J. Hansknecht and M. Poelker, "Synchronous Photoinjection using a Frequency-Doubled Gain-Switched Fiber-Coupled Seed Laser and ErYb-Doped Fiber Amplifier," *Phys. Rev. ST Accel. Beams* **9**, 063501 (2006).
- [11] T. Maruyama, D.-A. Luh, A. Brachmann, J.E. Clendenin, E.L. Garwin, S. Harvey, J. Jian, R.E. Kirby, C.Y. Prescott, R. Prepost, and A.M. Moy, "Systematic Study of Polarized Electron Emission from Strained GaAs/GaAsP Superlattice Photocathodes," *Appl. Phys. Lett.* **85**, 2640 (2004).
- [12] <https://en.wikipedia.org/wiki/Resonance> (last accessed 03/31/2019).
- [13] M. Cannon, "Blind Deconvolution of Spatially Invariant Image Blurs with Phase," *IEEE Trans. Acoust., Speech, Signal Process* **24**, 58 (1976).
- [14] E.Y. Lam and J.W. Goodman, Iterative statistical approach to blind image deconvolution, *JOSA A* **17**, 1177 (2000).
- [15] http://www.desy.de/~mpyflo/Astra_manual/Astra-Manual_V3.2.pdf (last accessed 03/31/2019).